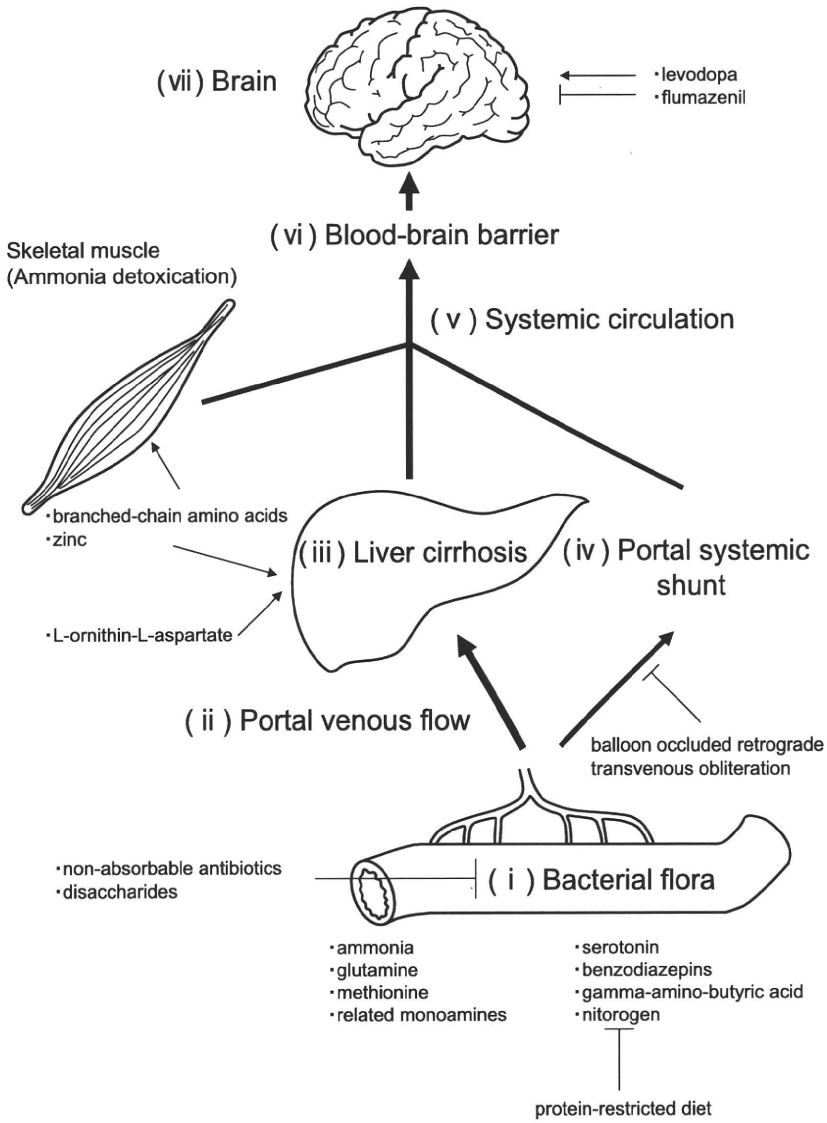

Figure 1 Pathophysiology of hepatic encephalopathy in liver cirrhosis, and action targets of therapeutic interventions. In patients with decompensated liver cirrhosis, (i) the endogenous neurotoxic substances are produced in the intestine by the bacterial flora, and (ii) are absorbed into the portal venous flow. They escape from catabolism by the liver, due both to (iii) the impaired function of the cirrhotic liver and also to (iv) the presence of portal systemic shunt. (v) These toxins then circulate at elevated concentrations in the systemic blood flow, (vi) reach the brain through the blood-brain barrier, and (vii) impair cerebral function leading to altered higher functions and consciousness. Therapeutic interventions either inhibit such pathophysiological pathways (⊥) or override (break down) the action of neurotoxins (vii). ←, levodopa; ⊢, flumazenil.

Table 1 Annual rate of occurrence of liver failure and its clinical symptoms in patients with liver cirrhosis, who have no past history of decompensation

	Annual rate	References
Hepatic failure (Total)	2–20%	10–14
Hepatic encephalopathy	8%	13
Ascites	7%	13
Edema	13%	13
Jaundice	9%	12

metabolic disorders such as hyperglycemia and hypoglycemia, and other organ failures, that is, the kidney, adrenal glands, and lung. In this context, it is important to note that the typical clinical sign of flapping tremor (asterixis) also appears in other disorders, such as hypoglycemia and renal insufficiency.

Supplemental clinical examinations for the diagnosis of hepatic encephalopathy are available, at first by psychometric tests such as the number connection test (NCT); this is particularly useful for the detection of minimal hepatic encephalopathy.[10,15,16] Medical imaging by computed tomography (CT)[17] and magnetic resonance

imaging (MRI)[18–22] usually show cerebral atrophy or, in acute type encephalopathy, cerebral edema. High-signal intensity of globus pallidus on MRI in liver cirrhosis is a famous sign, and is known to be brought about by manganese deposition. However, its specificity for hepatic encephalopathy is not yet definite, but rather seems to be due to portal systemic shunting.[18–21] Another MRI parameter, apparent diffusion coefficient (ADC) of water, has recently been reported as a reliable tool to quantify the grade of early hepatic encephalopathy in liver cirrhosis.[22] As an electrophysiological examination conventional electroencephalogram (EEG), shows slow waves with, sometimes, the appearance of triphasic wave. Somatosensory-evoked potential (SEP) is also useful.[23]

Epidemiology

Epidemiology of liver cirrhosis and hepatic encephalopathy

Epidemiology of liver cirrhosis depends particularly on the etiology, and shows a marked geographic difference worldwide, between Western, and Asian countries. While alcoholic consumption accounts for the majority in Western countries, hepatitis virus infection is the major cause of liver cirrhosis in the eastern hemisphere. In the latter region, hepatitis B virus (HBV) infection prevails on mainland Asia,[11] while two thirds of Japanese patients with cirrhosis are positive for hepatitis C virus (HCV).[24] Parasitic infection and intoxication with aflatoxin[25] in south-eastern Asia, and genetic disorders such as hemochromatosis[26] in Australia are also important causes of liver cirrhosis. The differences in the etiology of cirrhosis are significant with regard to the incidence of hepatocellular or cholangiocellular carcinoma, but no information is currently available on whether the development of hepatic encephalopathy depends on the cause of liver cirrhosis.

Incidence of hepatic encephalopathy

Studies on the incidence of liver failure in patients with liver cirrhosis, who have no past history of decompensation, are rare. Reliable longitudinal data in recently diagnosed with cirrhosis are available only in references #12, 20, 24, 25 and 26; the incidence ranges from 2% to 20%/year (Table 1). Among symptoms of decompensated cirrhosis, hepatic encephalopathy developed at an annual rate of 8% in one Japanese cohort.[13] Regarding the incidence of subclinical hepatic encephalopathy, a cross-sectional study of Child-Pugh grade A cirrhosis in China reported 40% had abnormal number connection test.[10]

Classification

Hepatic encephalopathy in liver cirrhosis is classified into two types; end-stage coma and chronic recurrent coma (Table 2).[1,13] These types are distinct in their prognosis, with poor survival rate in end-stage coma and favorable outcome for chronic recurrent encephalopathy (Table 2, Fig. 2). The precipitating factors in each type are listed in Table 2. The major cause of end-stage coma is massive gastrointestinal bleeding from ruptured esophageal varices or acute gastric mucosal lesion, while constipation/diarrhea, infection, and inappropriate use of diuretics are known to induce the chronic recurrent type. However, precipitating factors are unknown in approximately 30–40% of cases in both subtypes.

Table 2 Clinical subtypes of hepatic encephalopathy in liver cirrhosis (constructed based on the reference 13[13])

Subtype	End-stage coma	Chronic recurrent
Survival rate	23%	76%*
Precipitating factors	GI bleeding	Constipation/diarrhea
	Constipation/diarrhea	Infection
	Infection	Diuretics
	Renal failure	GI bleeding
		High protein diet
Duration (days)	13 (1–28)	3 (1–41)*
Maximum grade	IV	II*
Blood ammonia (ug/dL)	132	168
Prothrombin time (%)	43	54
Total bilirubin (mg/dL)	6	3*

Values are expressed as median.
*$P < 0.001$ as compared to end-stage coma.

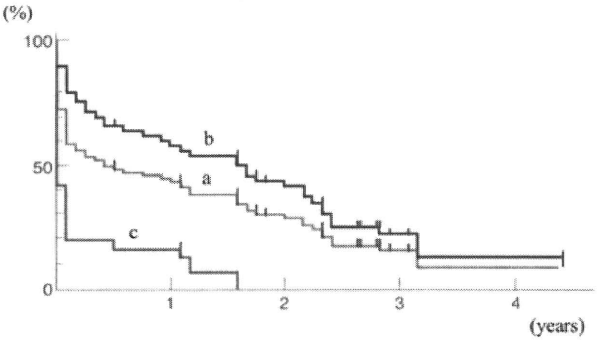

Figure 2 Survival rates of patients with liver cirrhosis from the initial episode of hepatic encephalopathy.[13] a. total, b, chronic recurrent type, and c, end-stage type hepatic encephalopathy.

Treatment

Candidate therapeutic modalities and interventions include protein- (or nitrogen-) restricted diet,[27–29] non-absorbable antibiotics,[30] oral disaccharides such as lactulose and lactitol,[31,32] disaccharide enema,[33] intravenous L-ornithine-L-aspartate (LOLA),[34] oral LOLA,[35] levodopa,[36] flumazenil,[37] intravenous or oral branched-chain amino acids (BCAA),[38–41] zinc supplementation,[42] portal-systemic shunt obliteration,[43] artificial liver support, and liver transplantation[44–46] (Fig. 1).

Among these therapeutics, first line treatment of hepatic encephalopathy in patients with liver cirrhosis has long been described as disaccharides, such as lactulose and lactitol.[1] However, recent studies including systematic reviews have questioned the effectiveness of this approach.[47–49] The most conservative statement in this regard at present is that treatment with lactulose/lactitol is effective at least against mild (including minimal) hepatic encephalopathy in cirrrhosis,[50] but seems to require additional or alternative approaches for overt encephalopathy.[51–53]

In Eastern and Far East countries, therapeutic options are similar to those described above, but pronounced application of dietary restriction, antimicrobial agents, and disaccharides is noted. In particular, Asian researchers have been involved in the clinical development of portal systemic shunt obliteration, that is balloon-occluded retrograde transvenous obliteration (BRTO).[43] Other characteristic interventions in the eastern hemisphere include intensive use of branched chain amino acid formulas.[39,54] The latter approach is also becoming popular in these countries particularly to prevent the development of liver failure, as described later. In parallel, these studies elucidated that the patients with cirrhosis already have major nutritional challenges, that is protein-energy malnutrition,[55,56] and require adequate nutritional support.[27,57] Thus, we should emphasize that protein restriction is not recommended generally by current guidelines as a treatment of cirrhotic encephalopathy,[27,57] but applied only for exceptional cases who show severe nitrogen-intolerance.

Comprehensive therapy is usually employed for hepatic encephalopathy because it appears as only one of a broad range of symptoms in liver failure. Focusing on this particular problem, the therapeutic efficacy as given by the arousal rate is shown in Table 2. For the chronic recurrent type of encephalopathy, response rates range from 70% to 100%,[1,13] but treatment efficacy is quite poor in the end-stage type of encephalopathy. However, even in the chronic recurrent type, repeated episodes bring deterioration of the patients' liver function reserve and also their general condition of encephalopathy, contributing to a low survival rate, 30% at 3 years (Fig. 2),[13] and 14% at 5 years.[46] This rate is similar to those reported in the Western hemisphere.[58] Thus, broader application of liver transplantation seems to be absolutely essential for the improvement of such poor long-term survival.[46]

Prevention

Another option to improve the poor general outcome after hepatic encephalopathy is the prevention of this type of consciousness disorder in patients with liver cirrhosis. In this regard, interventional radiology, such as BRTO to shut down the portal systemic shunt,[43] and endoscopic intervention for risky esophageal varices, are promising approaches. In addition, advances have been made in this century by applying oral (enteral) BCAA formulas in both Western,[59] Asian[60] and also Far Eastern research (Fig. 3).[12] The mechanism of action is agreed to be improvement of protein-energy malnutrition and recovery of general condition in the decompensated patients.[12,56,57] Detoxification of ammonia by BCAA in skeletal muscle seems an attractive hypothesis to explain the mechanism of action of BCAA,[61] but further basic, as well as clinical, studies require high priority.

Conclusions

Hepatic encephalopathy is still a serious complication of liver cirrhosis. In spite of improved therapeutic options for each episode, long-term survival still remains low. Establishment of truly effective prevention modalities and broader application of liver transplantation will help rescue patients suffering from this complication of liver cirrhosis in the near future. In preparing this manuscript, we made strenuous efforts to highlight characteristics of cirrhotic encephalopathy in Asia. However, insufficient clinical and experimental description is available, unfortunately, as can be seen from the number of references from Asian countries only 17 among a total of 61 articles cited. Further studies from the eastern hemisphere are absolutely waited to establish global agreement with regard to the wider clinical aspects for cirrhotic encephalopathy.

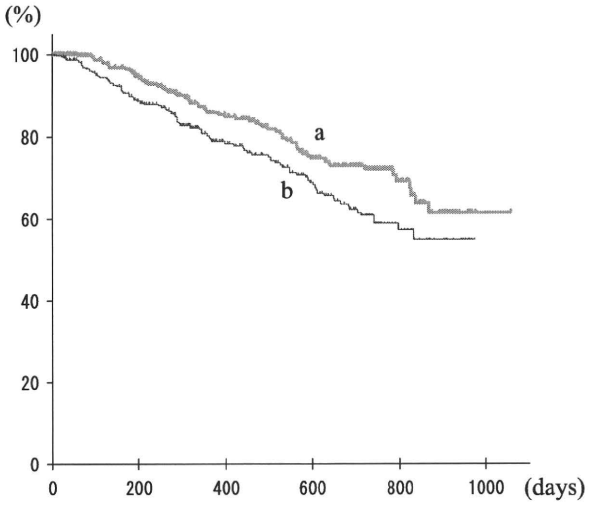

Figure 3 Effects of the oral supplementation with branched-chain amino acid granules on the event-free survival of patients with liver cirrhosis.[12] a, BCAA supplementation, b, control.

Acknowledgments

This work was supported in part by Grants-in-Aid for the Study Group for Intractable Liver Diseases and for the Study of Emerging and Reemerging Infectious Diseases from the Ministry of Health, Labor, and Welfare of Japan.

References

1 Sherlock S, Dooley J. Hepatic encephalopathy. In: Sherlock S, Dooley J, eds. *Diseases of the Liver and Biliary System*, 11th edn. Oxford: Blackwell Science, 2002; 87–102.
2 Plauth M, Roske A, Romaniuk P, Roth E, Ziebig R, Lochs H. Post-feeding hyperammonaemia in patients with transjugular intrahepatic portosystemic shunt and liver cirrhosis: role of small intestinal ammonia release and route of nutrient administration. *Gut* 2000; **46**: 849–55.
3 Mousseau DD, Butterworth RF. Current theories on the pathogenesis of hepatic encephalopathy. *Proc. Soc. Exp. Biol. Med.* 1994; **206**: 329–44.
4 Laubenberger J, Haussinger D, Bayer S, Gufler H, Hennig J, Langer M. Proton magnetic resonance spectroscopy of the brain in symptomatic and asymptomatic patients with liver cirrhosis. *Gastroenterology* 1997; **112**: 1610–16.
5 Mousseau DD, Baker GB, Butterworth RF. Increased density of catalytic sites and expression of brain monoamine oxidase A in humans with hepatic encephalopathy. *J. Neurochem.* 1997; **68**: 1200–8.
6 Mullen KD, Szauter KM, Kaminsky-Russ K. Endogenous

benzodiazepine activity in body fluids of patients with hepatic encephalopathy. *Lancet* 1990; **336**: 81–3.
7 Levy LJ, Leek J, Losowsky MS. Evidence for gamma-aminobutyric acid as the inhibitor of gamma-aminobutyric acid binding in the plasma of humans with liver disease and hepatic encephalopathy. *Clin. Sci. (Lond)* 1987; **73**: 531–4.
8 Ito Y, Nakamura T, Saito K *et al.* Pathophysiological role of intestinal flora in the Development of hepatic encephalopathy, with special reference to floral alterations induced by antimicrobial agents. *Microb. Ecol. Health Dis.* 1992; **5**: 1–13.
9 Ito Y, Moriwaki H, Muto Y, Kato N, Watanabe K, Ueno K. Effect of lactulose on short-chain fatty acids and lactate production and on the growth of faecal flora, with special reference to Clostridium difficile. *J. Med. Microbiol.* 1997; **46**: 80–4.
10 Li Y-Y, Nie Y-Q, Sha W-H *et al.* Prevalence of subclinical hepatic encephalopathy in cirrhotic patients in China. *World J. Gastroenterol.* 2004; **10**: 2397–401.
11 Yang SS, Wu CH, Chiang TR, Chen DS. Somatosensory evoked potentials in subclinical portosystemic encephalopathy: a comparison with psychometric tests. *Hepatology* 1998; **27**: 357–61.
12 Muto Y, Sato S, Watanabe A *et al.* Effects of oral branched-chain amino acid granules on event-free survival in patients with liver cirrhosis. *Clin. Gastroenterol. Hepatol.* 2005; **3**: 705–13.
13 Moriwaki H. Liver failure and hepatic encephalopathy. In: Sugimoto T, Yazaki Y, eds. *Textbook of Internal Medicine*, 9th edn. Tokyo: Asakura Shoten Co. Ltd., 2007; 933–6.
14 Lo KJ, Tong MJ, Chien MC *et al.* The natural course of hepatitis B surface antigen-positive chronic active hepatitis in Taiwan. *J. Infect. Dis.* 1982; **146**: 205–10.
15 Quero JC, Hartmann IJ, Meulstee J, Hop WC, Schalm SW. The diagnosis of subclinical hepatic encephalopathy in patients with cirrhosis using neuropsychological tests and automated electroencephalogram analysis. *Hepatology* 1996; **24**: 556–60.
16 Weissenborn K, Rückert N, Hecker H, Manns MP. The number connection tests A and B: interindividual variability and use for the assessment of early hepatic encephalopathy. *J. Hepatol.* 1998; **28**: 646–53.
17 Bernthal P, Hays A, Tarter RE, Van Thiel D, Lecky J, Hegedus A. Cerebral CT scan abnormalities in cholestatic and hepatocellular disease and their relationship to neuropsychologic test performance. *Hepatology* 1987; **7**: 107–14.
18 Rose C, Butterworth RF, Zayed J *et al.* Manganese deposition in basal ganglia structures results from both portal-systemic shunting and liver dysfunction. *Gastroenterology* 1999; **117**: 640–4.
19 Pomier-Layrargues G, Spahr L, Butterworth RF. Increased manganese concentrations in pallidum of cirrhotic patients. *Lancet* 1995; **345**: 735.
20 Nolte W, Wiltfang J, Schindler CG *et al.* Bright basal ganglia in T1-weighted magnetic resonance images are frequent in patients with portal vein thrombosis without liver cirrhosis and not suggestive of hepatic encephalopathy. *J. Hepatol.* 1998; **29**: 443–9.
21 Thuluvath PJ, Edwin D, Yue NC, deVilliers C, Hochman S, Klein A. Increased signals seen in globus pallidus in T1-weighted magnetic resonance imaging in cirrhotics are not suggestive of chronic hepatic encephalopathy. *Hepatology* 1995; **21**: 440–2.
22 Sugimoto R, Iwasa M, Maeda M *et al.* Value of the apparent diffusion coefficient for quantification of low-grade hepatic encephalopathy. *Am. J. Gastroenterol.* 2008; **103**: 1413–20.
23 Merican I, Guan R, Amarapuka D *et al.* Chronic hepatitis B virus infection in Asian countries. *J. Gastroenterol. Hepatol.* 2000; **15**: 1356–61.
24 Onji M. *Etiologies and Characteristics of Liver Cirrhosis in Japan 1998–2008*. Tokyo, Japan: Chugai Igaku Co. Ltd., 2008; 1–10.
25 El-Garem AA. Schistosomiasis. *Digestion* 1998; **59**: 589–605.
26 Merryweather-Clarke AT, Pointon JJ, Shearman JD, Robson KJ. Global prevalence of putative haemochromatosis mutations. *J. Med. Genet.* 1997; **34**: 275–8.
27 Plauth M, Cabre E, Riggio O *et al.* ESPEN guidelines on enteral nutrition: liver disease. *Clin. Nutr.* 2006; **25**: 285–94.
28 Mizock BA. Nutritional support in hepatic encephalopathy. *Nutrition* 1999; **15**: 220–8.
29 Cordoba J, Lopez-Hellin J, Planas M *et al.* Normal protein diet for episodic hepatic encephalopathy: results of a randomized study. *J. Hepatol.* 2004; **41**: 38–43.
30 Weber FL Jr, Fresard KM, Lally BR. Effects of lactulose and neomycin on urea metabolism in cirrhotic subjects. *Gastroenterology* 1982; **82**: 213–17.
31 Morgan MY, Hawley KE. Lactitol vs. lactulose in the treatment of acute hepatic encephalopathy in cirrhotic patients: a double-blind, randomized trial. *Hepatology* 1987; **7**: 1278–84.
32 Trovato GM, Catalano D, Carpinteri G, Runcio N, Mazzone O. Effects of lactitol [correction of lactilol] on hepatic encephalopathy and plasma amino-acid imbalance. *Recenti. Prog. Med.* 1995; **86**: 299–303.
33 Uribe M, Campollo O, Vargas F *et al.* Acidifying enemas (lactitol and lactose) *vs.* nonacidifying enemas (tap water) to treat acute portal-systemic encephalopathy: a double-blind, randomized clinical trial. *Hepatology* 1987; **7**: 639–43.
34 Kircheis G, Nilius R, Held C *et al.* Therapeutic efficacy of L-ornithine-L-aspartate infusions in patients with cirrhosis and hepatic encephalopathy: results of a placebo-controlled, double-blind study. *Hepatology* 1997; **25**: 1351–60.
35 Stauch S, Kircheis G, Adler G *et al.* Oral L-ornithine-L-aspartate therapy of chronic hepatic encephalopathy: results of a placebo-controlled double-blind study. *J. Hepatol.* 1998; **28**: 856–64.
36 Lunzer M, James IM, Weinman J, Sherlock S. Treatment of chronic hepatic encephalopathy with levodopa. *Gut* 1974; **15**: 555–61.
37 Barbaro G, Di Lorenzo G, Soldini M *et al.* Flumazenil for hepatic encephalopathy grade III and IVa in patients with cirrhosis: an Italian multicenter double-blind, placebo-controlled, cross-over study. *Hepatology* 1998; **28**: 374–8.
38 Morgan MY. Branched chain amino acids in the management of chronic liver disease. Facts and fantasies. *J. Hepatol.* 1990; **11**: 133–41.
39 Suzuki K, Kato A, Iwai M. Branched-chain amino acid treatment in patients with liver cirrhosis. *Hepatol. Res.* 2004; **30S**: 25–9.
40 Fabbri A, Magrini N, Bianchi G, Zoli M, Marchesini G. Overview of randomized clinical trials of oral branched-chain amino acid treatment in chronic hepatic encephalopathy. *JPEN J .Parenter. Enteral. Nutr.* 1996; **20**: 159–64.
41 Calvey H, Davis M, Williams R. Controlled trial of nutritional supplementation, with and without branched chain amino acid enrichment, in treatment of acute alcoholic hepatitis. *J. Hepatol.* 1985; **1**: 141–51.
42 Marchesini G, Fabbri A, Bianchi G, Brizi M, Zoli M. Zinc supplementation and amino acid-nitrogen metabolism in patients with advanced cirrhosis. *Hepatology* 1996; **23**: 1084–92.
43 Kawanaka H, Ohta M, Hashizume M *et al.* Portosystemic encephalopathy treated with balloon-occluded retrograde transvenous obliteration. *Am. J. Gastroenterol.* 1995; **90**: 508–10.
44 Parkes JD, Murray-Lyon IM, Williams R. Neuropsychiatric and electro-encephalographic changes after transplantation of the liver. *Q. J. Med.* 1970; **39**: 515.
45 Powell EE, Pender MP, Chalk JB *et al.* Improvement in chronic hepatocerebral degeneration following liver transplantation. *Gastroenterology* 1990; **98**: 1079–82.
46 de Jonah FE, Janssen HL, de Man RA *et al.* Survival and prognostic

indicators in hepatitis B surface antigen-positive cirrhosis of the liver. *Gastroenterology* 1992; **103**: 1692–4.
47 Als-Nielsen B, Gluud LL, Gluud C. Nonabsorbable disaccharides for hepatic encephalopathy. *Cochrane Database Syst. Rev.* 2004: 1–65.
48 Als-Nielsen B, Gluud LL, Gluud C. Non-absorbable disaccharides for hepatic encephalopathy: systematic review of randomised trials. *BMJ* 2004; **328**: 1046.
49 Shawcross D, Jalan R. Dispelling myths in the treatment of hepatic encephalopathy. *Lancet* 2005; **365**: 431–3.
50 Prasad S, Dhiman RK, Duseja A, Chawla YK, Sharma A, Agarwal R. Lactulose improves cognitive functions and health-related quality of life in patients with cirrhosis who have minimal hepatic encephalopathy. *Hepatology* 2007; **45**: 549–59.
51 Larsen FS, Wendon J. Alternative pathway therapy for hyperammonemia in liver failure. *Hepatology* 2009; **50**: 3–5.
52 Davies NA, Wright G, Ytrebø LM *et al.* L-ornithine and phenylacetate synergistically produce sustained reduction in ammonia and brain water in cirrhotic rats. *Hepatology* 2009; **50**: 155–64.
53 Ytrebø LM, Kristiansen RG, Maehre H *et al.* L-ornithine phenylacetate attenuates increased arterial and extracellular brain ammonia and prevents intracranial hypertension in pigs with acute liver failure. *Hepatology* 2009; **50**: 165–74.
54 Iwasa M, Matsumura K, Watanabe Y *et al.* Improvement of regional cerebral blood flow after treatment with branched-chain amino acid solutions in patients with cirrhosis. *Eur. J. Gastroenterol. Hepatol.* 2003; **15**: 733–7.
55 Alberino F, Gatta A, Amodio P *et al.* Nutrition and survival in patients with liver cirrhosis. *Nutrition* 2001; **17**: 445–50.
56 Tajika M, Kato M, Mohri H *et al.* Prognostic value of energy metabolism in patients with viral liver cirrhosis. *Nutrition* 2002; **18**: 229–34.
57 ASPEN Board of Directors and the Clinical Guidelines Task Force. Guidelines for the use of parenteral and enteral nutrition in adult and pediatric patients. *J. Parenter. Enteral. Nutr.* 2002; **26** (Suppl.): 73–5.
58 Bustamante J, Rimola A, Ventura PJ *et al.* Prognostic significance of hepatic encephalopathy in patients with cirrhosis. *J. Hepatol.* 1999; **30**: 890–5.
59 Marchesini G, Bianchi G, Merli M *et al.* Italian BCAA Study Group. Nutritional supplementation with branched-chain amino acids in advanced cirrhosis: a double-blind, randomized trial. *Gastroenterology* 2003; **124**: 1792–801.
60 Poon RT, Yu WC, Fan ST, Wong J. Long-term oral branched chain amino acids in patients undergoing chemoembolization for hepatocellular carcinoma: a randomized trial. *Aliment. Pharmacol. Ther.* 2004; **19**: 779–88.
61 Hayashi M, Ohnishi H, Kawade Y, Muto Y, Takahashi Y. Augmented utilization of branched-chain amino acids by skeletal muscle in decompensated liver cirrhosis in special relation to ammonia detoxication. *Gastroenterol. Jpn.* 1981; **16**: 64–70.

Ability of IDO To Attenuate Liver Injury in α-Galactosylceramide–Induced Hepatitis Model

Hiroyasu Ito,* Masato Hoshi,* Hirofumi Ohtaki,* Ayako Taguchi,† Kazuki Ando,*,‡ Tetsuya Ishikawa,§ Yosuke Osawa,* Akira Hara,† Hisataka Moriwaki,¶ Kuniaki Saito,‖ and Mitsuru Seishima*

IDO converts tryptophan to L-kynurenine, and it is noted as a relevant molecule in promoting tolerance and suppressing adaptive immunity. In this study, we examined the effect of IDO in α-galactosylceramide (α-GalCer)–induced hepatitis. The increase in IDO expression in the liver of wild-type (WT) mice administered α-GalCer was confirmed by real-time PCR, Western blotting, and IDO immunohistochemical analysis. The serum alanine aminotransferase levels in IDO-knockout (KO) mice after α-GalCer injection significantly increased compared with those in WT mice. 1-Methyl-D-tryptophan also exacerbated liver injury in this murine hepatitis model. In α-GalCer–induced hepatitis models, TNF-α is critical in the development of liver injury. The mRNA expression and protein level of TNF-α in the liver from IDO-KO mice were more enhanced compared with those in WT mice. The phenotypes of intrahepatic lymphocytes from WT mice and IDO-KO mice treated with α-GalCer were analyzed by flow cytometry, and the numbers of CD49b$^+$ and CD11b$^+$ cells were found to have increased in IDO-KO mice. Moreover, as a result of the increase in the number of NK cells and macrophages in the liver of IDO-KO mice injected with α-GalCer, TNF-α secretion in these mice was greater than that in WT mice. Deficiency of IDO exacerbated liver injury in α-GalCer–induced hepatitis. IDO induced by proinflammatory cytokines may decrease the number of TNF-α–producing immune cells in the liver. Thus, IDO may suppress overactive immune response in the α-GalCer–induced hepatitis model. ***The Journal of Immunology*****, 2010, 185: 4554–4560.**

Indoleamine 2,3-dioxygenase has been identified as an enzyme that has powerful immunomodulatory effects, resulting from its enzymatic activity, which leads to catabolism of the essential amino acid L-tryptophan (L-Trp) to L-kynurenine (L-Kyn) (1, 2). This enzyme is expressed in epithelial, macrophage, and dendritic cells induced by proinflammatory cytokines, including type I and type II IFN (3, 4). The binding of CTLA-4 with CD80/CD86 on the membrane of dendritic cells also stimulates IDO transcriptional expression and activity (5, 6). Furthermore, metabolites of the L-Kyn pathway have been shown to act as immunoregulatory molecules that have immunosuppressive effects in the tissue microenvironment (7). IDO and the L-Trp pathway play critical roles in the generation of immune tolerance against foreign Ags in tissue microenvironments. Recently, we demonstrated that IDO expression on hepatocytes is increased in liver injury caused by hepatitis B virus-specific CTL in hepatitis B virus transgenic mice (8). Furthermore, it has been reported that IDO expressions in the liver and serum L-Kyn/L-Trp ratios in patients with chronic hepatitis C were increased and that this upregulation of IDO was caused by the IFN-γ produced by hepatitis C virus-activated T cells in the liver (9). As shown above, IDO expression is significantly enhanced during liver injury. We therefore established two hypotheses on the role of IDO: 1) IDO directly or indirectly brings about the progression of liver injury; and 2) IDO production is enhanced as a protective mechanism in liver injury. However, the actual role of IDO in liver injury remains unknown.

Several reports have demonstrated that α-galactosylceramide (α-GalCer), a specific ligand for invariant Vα14 NKT cells, induces liver injury (10–12). α-GalCer is hepatotoxic since the administration of α-GalCer in mice results in the activation and apoptosis of hepatic Vα14 NKT cells via activation-induced cell death and associated liver damage. Furthermore, the hepatotoxic effect of α-GalCer was found to be mediated by TNF-α produced by activated hepatic Vα14 NKT cells (12). In fact, it was proposed that TNF-α increases FasL expression on Vα14 NKT cells, and that these cells in turn promote liver damage by interacting with Fas-expressing hepatocytes (12). It is noteworthy that liver injury induced by α-GalCer is thought to potentially mimic some aspects of autoimmune hepatitis. The liver appears to be particularly susceptible to injury as a result of increased immune responses, mainly mediated by T lymphocytes and/or emerging autoantibodies. On viral infection of hepatocytes, the cytopathic effect of the virus per se is only moderate; instead, liver damage is caused by cellular immune responses to infected cells. Thus, the host immune system is related to the initiation and progression of liver injury in several liver injury models, and it is very important to determine the role of IDO and its powerful immunomodulatory effects during hepatic injury.

In this study, we examined the effect of IDO on α-GalCer–induced liver injury in mice and demonstrated that liver injury was exacerbated in IDO-deficient mice.

*Department of Informative Clinical Medicine, †Department of Tumor Pathology, and ¶First Department of Internal Medicine, Gifu University Graduate School of Medicine, Gifu; ‡Goto Clinic, Ogaki; §Cancer Immunotherapy Center, Nagoya Kyoritsu Hospital, Nagoya; and ‖Human Health Science, Graduate School of Medicine and Faculty of Medicine, Kyoto University, Kyoto, Japan

Received for publication December 28, 2009. Accepted for publication August 9, 2010.

Address correspondence and reprint requests to Dr. Hiroyasu Ito, Department of Informative Clinical Medicine, Gifu University Graduate School of Medicine, 1-1 Yanagido, Gifu 501-1194, Japan. E-mail address: hito@gifu-u.ac.jp

Abbreviations used in this paper: ALT, alanine aminotransferase; α-GalCer, α-galactosylceramide; IHL, intrahepatic lymphocyte; KC, keratinocyte chemoattractant; KO, knockout; L-Kyn, L-kynurenine; L-Trp, L-tryptophan; MNC, mononuclear cell; 1-MT, 1-methyl-D-tryptophan; WT, wild-type.

 0022-1767/10/$16.00

www.jimmunol.org/cgi/doi/10.4049/jimmunol.0904173

Materials and Methods

Mice

Male C57BL/6J wild-type (WT) mice (age, 8–10 wk; weight, 25–30 g) were obtained from Japan SLC (Shizuoka, Japan). IDO-knockout (KO) mice with a C57BL/6J background were obtained from The Jackson Laboratory (Bar Harbor, ME). All procedures were conducted in accordance with the National Institutes of Health Guide for the Care and Use of Laboratory Animals, and with the guidelines for the care and use of animals established by the Animal Care and Use Committee of Gifu University.

Animal treatment

α-GalCer was obtained from Funakoshi (Tokyo, Japan) and stored as a 200 μg/ml stock solution in vehicle (0.5% w/v polysorbate-20); it was then diluted in pyrogen-free saline to obtain the indicated dose directly before i.v. injection of a total volume of 200 μl/mouse. Hepatocellular injury was monitored biochemically through measurement of serum alanine aminotransferase (ALT) activity. At appropriate time points, mice were killed by cervical dislocation, and necropsy was performed. Tissue samples were fixed in 10% formalin, embedded in paraffin, and sectioned; the sections were then stained with H&E.

Immunohistochemical analysis

Tissues were fixed in 10% formalin in PBS overnight. Specimens were then embedded in paraffin. Sections that were 4 μm thick were used for H&E staining and immunohistochemical analysis for IDO as described previously (13). For the immunohistochemical analysis, the deparaffinized sections were heated in 0.1 M citrate buffer (pH 6.0), using the Pascal heat-induced target retrieval system (Dako, Carpinteria, CA). Nonspecific Ab binding sites were blocked in PBS (pH 7.4) containing 2% BSA (Wako Pure Chemical Industries, Osaka, Japan) for 60 min. The sections were then incubated with rabbit anti-IDO polyclonal Ab (anti-mouse IDO Ab was generated by the peptide H-CMKPSKKKPTDGDKS-OH) diluted 1/100 in 2% BSA/PBS and incubated overnight at 4°C. The IDO protein was shown by using a labeled streptavidin-biotin kit (Dako Japan, Kyoto, Japan) containing biotinylated Ab and peroxidase-labeled streptavidin. The peroxidase binding sites were detected by staining with 3,3′-diaminobenzidine. Finally, counterstaining was performed using Mayer's hematoxylin.

Determination of L-Kyn concentrations

Plasma from the mice was mixed with 3 volumes of 3% perchloric acid. After centrifugation, the concentrations of L-Kyn in the supernatants were measured using HPLC with a 5-mm octyldecylsilane column (150 × 2.1 mm; Eicom, Kyoto, Japan) and a spectrophotometric detector or a fluorescence spectrometric detector as described previously (13). UV signals were monitored at 355 nm for L-Kyn. The mobile phase consisted of 2.5% acetonitrile in 0.1 M sodium acetate (pH 3.9) and was filtered through a 0.45-μm-pore HA-type filter obtained from Millipore (Bedford, MA). The flow rate was maintained at 0.75 ml/min throughout the chromatographic run.

Analysis of liver transaminase

Hepatocyte damage was assessed at the indicated time points after α-GalCer injection through measurement of plasma ALT activities using an automated clinical analyzer (BM2250; JEOL, Tokyo, Japan).

Hepatic mononuclear cell preparation and flow cytometric analysis

Hepatic mononuclear cells (MNCs) were isolated and purified as previously described (14). Briefly, the excised liver was cut into small pieces with scissors, pressed through a 200-gauge stainless mesh, and suspended in PBS. Lymphocytes were separated from parenchymal hepatocytes and hepatocyte nuclei by Ficoll-Conray (IBL, Gunma, Japan) and washed twice in ice-cold medium. Cell viability and cell numbers were assessed by trypan blue exclusion. For flow cytometry, 2×10^5 liver MNCs were stained using a standard protocol. The following Abs were used: FITC-labeled hamster anti-mouse CD3ε mAb (clone 145-2c11), FITC-labeled rat anti-mouse CD4 mAb (clone RM4-5), FITC-labeled rat anti-mouse Gr-1 mAb (clone RB6-8C5), PE-labeled rat anti-mouse CD49b mAb (clone DX5), PE-labeled rat anti-mouse CD8a mAb (clone 53-6.7), and PE-labeled rat anti-mouse CD11b mAb (clone M1/70) (all from eBioscience, San Diego, CA). Samples were acquired on a FACStar flow cytometer, and data analysis was performed using CellQuest software (BD Biosciences, San Jose, CA).

Isolation of mouse hepatocytes

The abdomen of a sacrificed mouse was opened and a needle was inserted into the vena cava. The portal vein was punctured. The liver was perfused with PBS and liver perfusion medium (Invitrogen Life Technologies, Carlsbad, CA). To obtain nonparenchymal cell populations, the liver was perfused with liver digestion medium (Invitrogen Life Technologies), removed, and gently pressed through a mesh. Nonparenchymal cell were separated from parenchymal hepatocytes by centrifugation at 50 × *g* for 5 min. The purified cell population obtained in the final cell pellet was composed of ≥96% hepatocytes as previously reported (15).

Real-time PCR

Total RNA was isolated and transcribed into cDNA with an RNeasy Mini kit (Qiagen, Hilden, Germany) and High-Capacity cDNA Reverse Transcription kits (Applied Biosystems, Foster City, CA). The resulting cDNA was used as a template for real-time PCR along with primer/probe sets for IDO, TNF-α, IL-2, IL-4, IL-6, IL-10, IFN-γ, MCP-1, MIP-2, keratinocyte chemoattractant (KC), and TGF-β (TaqMan Gene Expression Assays; Applied Biosystems) and 2× TaqMan Universal PCR Master Mix (Applied Biosystems) according to the manufacturer's recommendations. The primer/probe sets for 18S were used as internal controls in the reactions (Applied Biosystems). Real-time PCR data were analyzed using sequence detector software (Applied Biosystems).

Western blot analysis

Protein (20 μg) from the cell lysate was subjected to SDS-PAGE and transferred to nitrocellulose membranes. After blocking nonspecific reactions with 5% skim milk, the membrane was incubated with anti-IDO and anti-GAPDH Abs for 60 min at room temperature and subsequently incubated with peroxidase-labeled anti-mouse or -rabbit IgG Ab for 60 min at room temperature. Immunoreactive protein bands were visualized with ECL Plus (GE Healthcare, Buckinghamshire, U.K.).

Cytokine and chemokine detection by ELISA

The concentrations of circulating TNF-α, IL-6, MIP-2, and KC in the sera were determined by an ELISA kit (R&D Systems, Minneapolis, MN), according to the manufacturer's instructions. The experimental results are expressed as the mean of triplicates (±SD) of three independent experiments.

Intracellular cytokine staining

For intracellular staining, hepatic MNCs from the mice that were administered α-GalCer were incubated for 4 h with brefeldin A (10 μg/ml). Then these cells were fixed, permeabilized with the Cytofix/Cytoperm buffer (BD Pharmingen, San Diego, CA), and stained with FITC-conjugated anti-mouse TNF-α (clone MP6-XT22; eBioscience). Samples were acquired on a FACStar flow cytometer, and data analysis was conducted using the CellQuest software (BD Biosciences).

Statistical analysis

Values are expressed as means (SEM). Differences between the experimental and control groups were analyzed by the Kruskal-Wallis test followed by the Scheffé *F* test. Significance was established at $p < 0.05$.

Results

Upregulation of IDO expression and activity in the liver after α-GalCer injection

We studied the increase in IDO in the liver as a result of α-GalCer treatment. As shown in Fig. 1*A*, to assess the changes in IDO activity in the WT and IDO-KO mice treated with α-GalCer, we first investigated the time course of changes in the serum L-Kyn concentration. The serum L-Kyn levels in WT mice were significantly increased at least as early as 20 h following α-GalCer (2 μg/mouse) injection compared with those in IDO-KO mice, and this increase in serum L-Kyn levels persisted on day 7 after α-GalCer injection. We next examined both IDO mRNA expression and IDO protein levels in the liver of WT and IDO-KO mice administered α-GalCer (Fig. 1*B–D*). IDO mRNA expression in the liver of WT mice was significantly increased at 24 h after α-GalCer injection. Western blot analysis and immunohistochemical examination revealed that the IDO protein levels in the livers from WT mice were upregulated

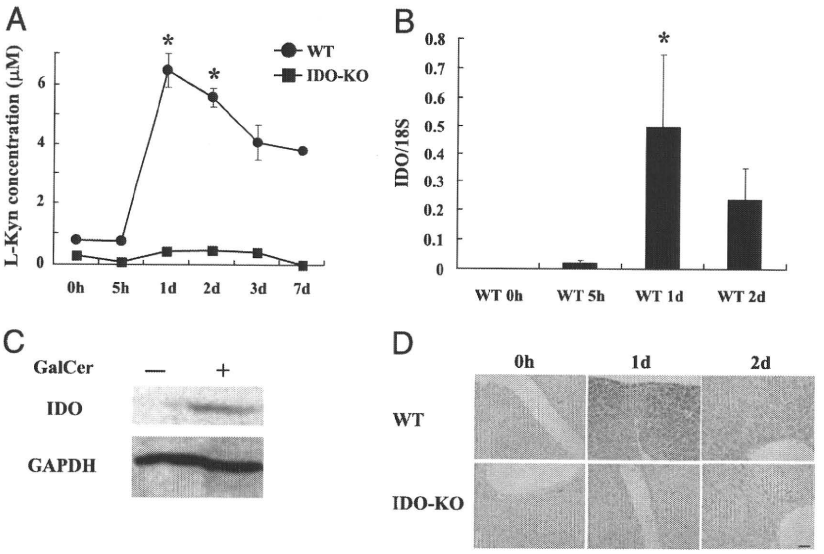

FIGURE 1. Upregulation of IDO expression and activity in the liver after α-GalCer injection. *A*, L-Kyn concentrations in serum determined by performing the HPLC method on WT and IDO-KO mice treated with α-GalCer. Each value is represented by the mean (SEM) of three mice. $*p < 0.05$. *B*, The relative expression levels of IDO mRNA in the livers of WT mice administered α-GalCer were measured using quantitative real-time PCR. The results were normalized by the expression of 18S mRNA. Each value is represented by the mean (SEM) of three mice. $*p < 0.05$. *C*, Expression of IDO protein in the livers of WT mice 1 d after treatment with α-GalCer was examined by Western blot analysis and was determined using the GAPDH protein. Data are representative of at least three independent experiments with similar results. *D*, Immunohistochemical analysis of IDO in the liver of WT and IDO-KO mice after α-GalCer injection. IDO protein was stained by using a labeled streptavidin-biotin kit containing biotinylated Ab and peroxidase-labeled streptavidin. The peroxidase binding sites were detected by staining with 3,39-diaminobenzidine. Scale bar, 25 μm. Original magnification ×200. Data are representative of at least three independent experiments with similar results.

after α-GalCer injection. This increase in IDO expression was observed in hepatocytes in particular.

Induction of liver injury by α-GalCer in WT mice and IDO-KO mice

To determine whether IDO plays a critical role in α-GalCer–induced liver injury, IDO-KO mice and WT mice were i.v. injected with α-GalCer (2 μg/mouse). Serum ALT activity started increasing at 12 h, reached a peak at 1 d, and returned to normal at 5 d after injection in WT mice (Fig. 2*A*). Surprisingly, serum ALT activity in IDO-KO mice significantly increased at 1 and 2 d after the injection compared with the activity in WT mice. To examine histological changes in the liver in the presence or absence of IDO after α-GalCer injection, we subjected liver tissues to H&E staining. As shown in Fig. 2*B*, livers from both WT and IDO-KO mice were mostly histologically normal except for a few very small and widely scattered necroinflammatory foci consisting of lymphomononuclear cells and apoptotic hepatocytes 1 d after α-GalCer injection. At 2 d after α-GalCer injection, the necroinflammatory foci in the livers of IDO-KO mice became larger and more abundant compared with those in WT mice, consisting of a mixed population of lymphomononuclear cells and apoptotic hepatocytes that often displayed granulomatous features in the hepatic parenchyma.

α-GalCer–induced TNF-α production in WT and IDO-KO mice

It was previously reported that neutralization of TNF-α significantly reduced induced α-GalCer–induced hepatic injury (12); in fact, TNF-α is thought to play a critical role in α-GalCer–induced liver injury. Therefore, we next examined TNF-α production in WT and IDO-KO mice treated with α-GalCer. TNF-α mRNA expression in the livers of IDO-KO mice was increased compared with that in the livers of WT mice at 12 h after α-GalCer treatment (Fig. 3*A*). Moreover, we measured plasma TNF-α levels up to 2 d after administration of 2 μg of α-GalCer to WT and IDO-KO mice by ELISA (Fig. 3*B*). The TNF-α levels peaked at 5 h after α-GalCer application in both WT mice and IDO-KO mice. How-

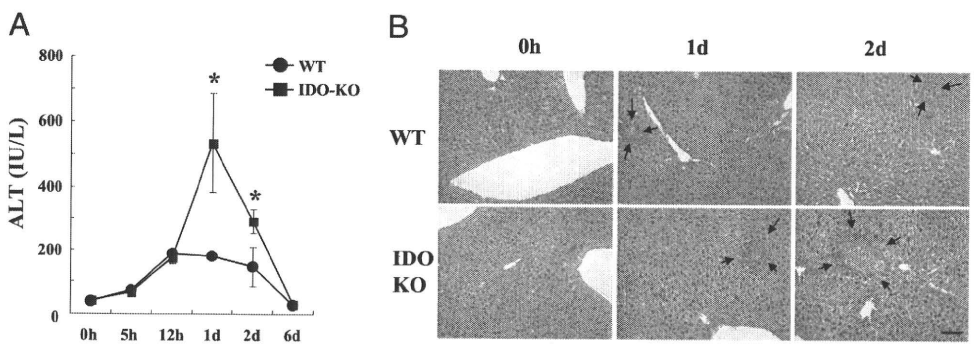

FIGURE 2. Induction of liver injury by α-GalCer in WT mice and IDO-KO mice. *A*, Serum ALT activity was measured at varying time points after α-GalCer injection into WT and IDO-KO mice. Each value is represented by the mean (SEM) of three mice. $*p < 0.05$. *B*, Histopathological characteristics of WT and IDO-KO mice livers observed at 0, 1, and 2 d after α-GalCer administration in these mice. H&E, original magnification ×200; scale bar, 100 μm. Arrows designate necroinflammatory foci in the liver. These experiments were repeated three times, and the same results were obtained.

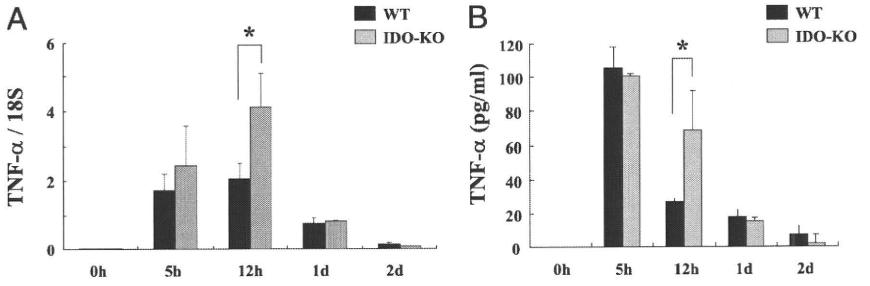

FIGURE 3. α-GalCer–induced TNF-α production in WT and IDO-KO mice. *A*, TNF-α mRNA expression in the livers of WT and IDO-KO mice that were administered α-GalCer. The mRNA level of TNF-α was normalized to that of 18S mRNA. Representative charts were derived from the analyses of three mice per group. *B*, Serum TNF-α concentration was determined by ELISA in WT and IDO-KO mice after α-GalCer injection. Each value is represented by the mean (SEM) of three mice. $*p < 0.05$.

ever, the concentration of TNF-α in IDO-KO mice was significantly increased compared with that in WT mice at 12 h after α-GalCer injection.

α-GalCer–induced cytokine and chemokine expression in WT mice and IDO-KO mice

As reported previously, NKT cells can produce a broad range of immunostimulatory or immunoregulatory cytokines and chemokines on activation, such as IL-2, IL-4, IL-10, IFN-γ, TNF-α, MIP-2, and KC (16–18). Therefore, we conducted a detailed time course analysis of the mRNA expression of intrahepatic cytokines (IFN-γ, IL-2, IL-4, IL-6, IL-10, and TGF-β) and chemokines (MIP-2, MCP-1, and KC) in WT and IDO-KO mice treated with α-GalCer (Fig. 4). Intrahepatic IL-6, MIP-2, and KC mRNA expression in IDO-KO mice was significantly increased compared with that in WT mice at 12 h after α-GalCer treatment. The marked differences between WT and IDO-KO mice were not observed with the mRNA expression of other cytokines and chemokines. Next, we measured the serum IL-6, MIP-2, and KC concentrations in WT and IDO-KO mice treated with α-GalCer. Although intrahepatic mRNA expressions of these

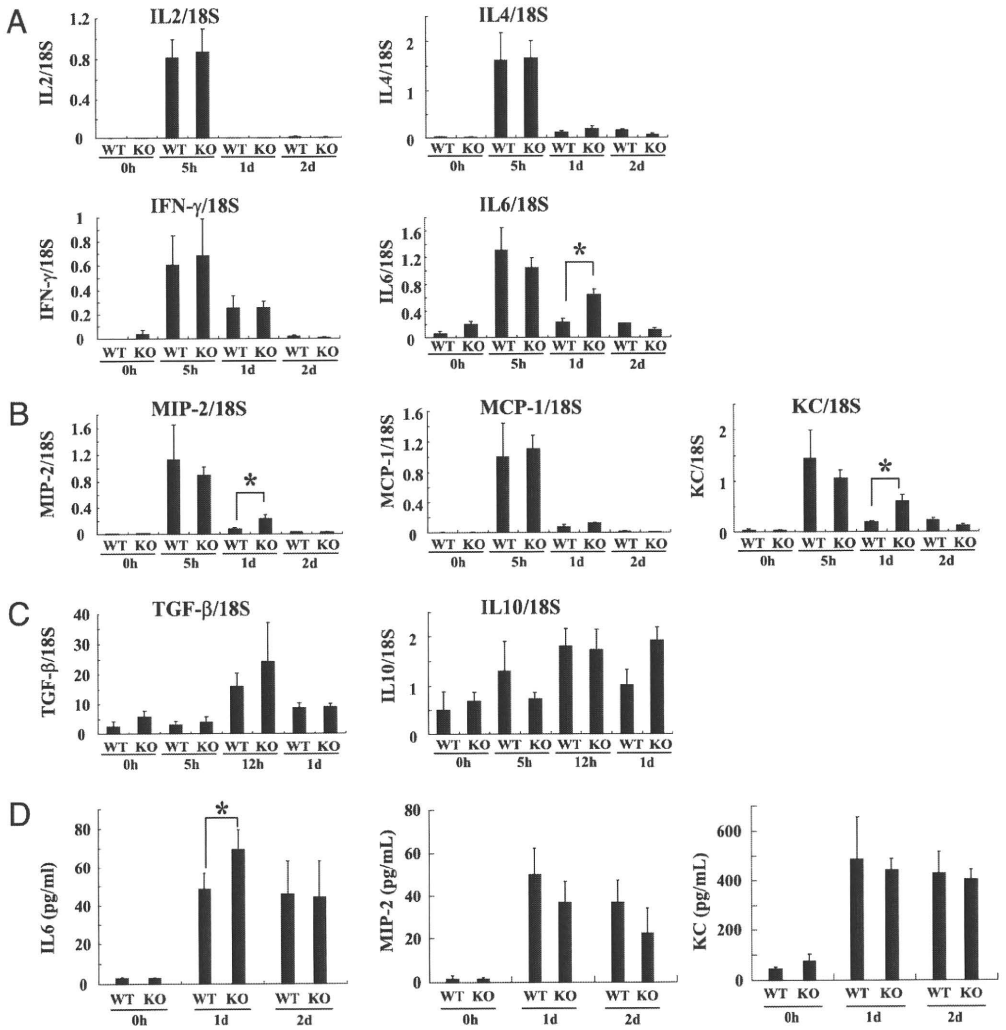

FIGURE 4. α-GalCer–induced cytokine and chemokine expression in WT mice and IDO-KO mice. *A*, IL-2, IL-4, IL-6, and IFN-γ mRNA expression in the livers of WT and IDO-KO mice that were administered α-GalCer. *B*, mRNA expression of chemokines (MIP-2, MCP-1, and KC) in the livers of WT and IDO-KO mice that were administered α-GalCer. *C*, TGF-β and IL-10 mRNA expression in the livers of WT and IDO-KO mice that were administered α-GalCer. The mRNA levels of cytokines and chemokines were normalized to those of 18S mRNA. *D*, Serum IL-6, MIP-2, and KC concentrations in WT and IDO-KO mice after α-GalCer injection were determined by ELISA. Representative charts derived from the analyses of three mice per group. $*p < 0.05$.

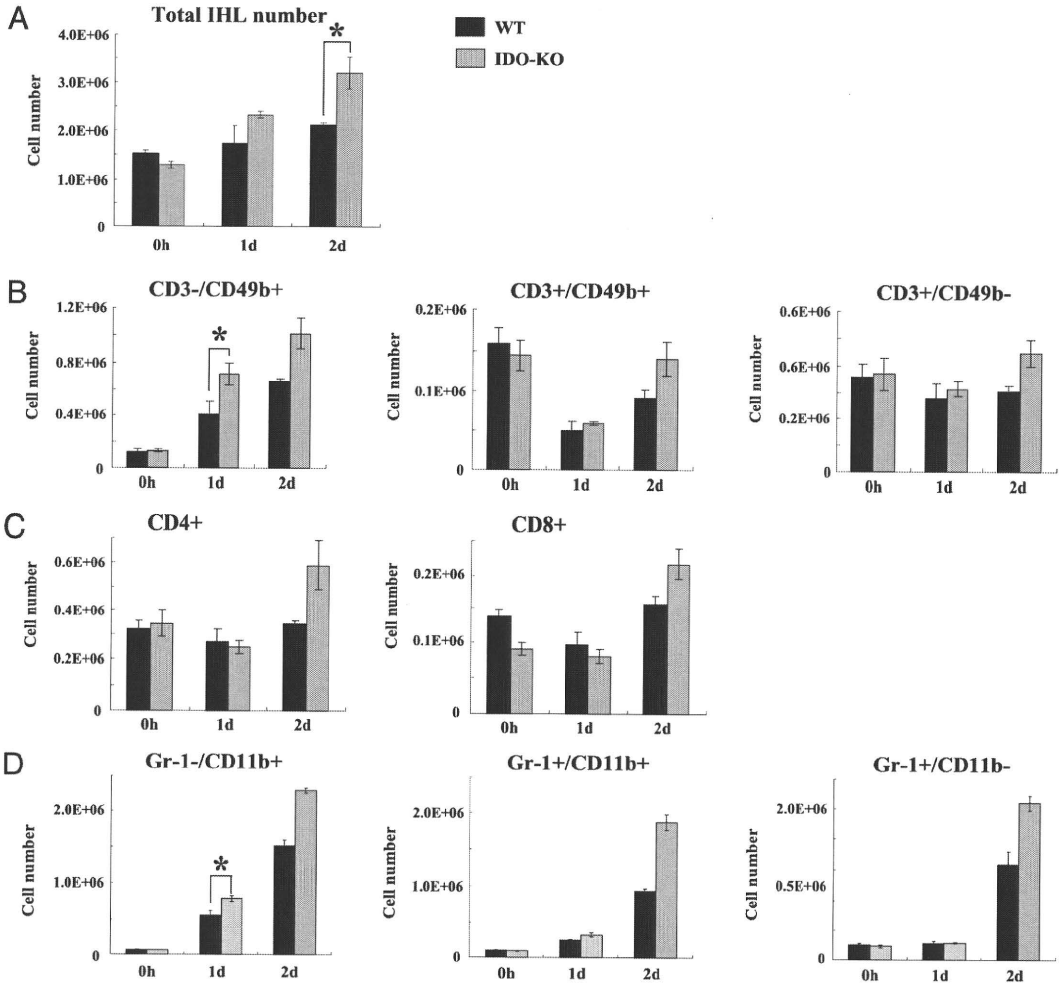

FIGURE 5. Kinetics and lymphocyte phenotypes of hepatic MNCs after α-GalCer injection into WT and IDO-KO mice. Hepatic MNCs from WT (black bars) and IDO-KO (gray bars) mice were obtained at 0, 1, and 2 d after α-GalCer injection. Cell numbers were quantified using FACScan analysis. *A*, Total number of hepatic MNCs after α-GalCer injection. *B*, Number of $CD3^-CD49b^+$ cells, $CD3^+CD49b^+$ cells, and $CD3^+CD49b^-$ cells after α-GalCer injection. *C*, Number of $CD4^+$ and $CD8^+$ cells after α-GalCer injection. *D*, Number of $CD11b^+Gr\text{-}1^-$ cells, $CD11b^+Gr\text{-}1^+$ cells, and $CD11b^-Gr\text{-}1^+$ cells at 1 d after α-GalCer injection. Results are presented as the mean number of cells of each cell type of hepatic MNCs for at least three mice per group. Error bars indicate the SEM. $*p < 0.05$. IHL, intrahepatic lymphocyte.

chemokines and cytokine in IDO-KO mice were increased compared with those in WT mice, the concentration of IL-6 in IDO-KO mice only elevated in serum.

Lymphocyte phenotypes of hepatic MNCs after α-GalCer injection into WT and IDO-KO mice

Next, we examined the lymphocyte phenotypes of hepatic MNCs from WT and IDO-KO mice treated with α-GalCer. The total number of MNCs in the livers of WT mice and IDO-KO mice was increased after α-GalCer injection. The increase in cell number was more enhanced in IDO-KO mice compared with WT mice at 2 d after α-GalCer injection (Fig. 5*A*). In particular, the frequency of hepatic $CD49b^+$ cells in IDO-KO mice significantly increased at 1 d after α-GalCer injection (Fig. 5*B*), coinciding with the peak of serum (Fig. 2). Although the number of $CD4^+$ and $CD8^+$ cells in the liver of IDO-KO mice increased compared with that in WT mice, the peak time was delayed compared with the peak time of liver injury in this model (Fig. 5*C*). Moreover, we measured the number of monocytes/macrophages in the liver from WT and IDO-KO mice after α-GalCer injection (Fig. 5*D*). The number of $CD11b^+Gr\text{-}1^-$ cells from IDO-KO mice was significantly increased compared with that from WT mice.

α-GalCer–induced TNF-α production in $CD49b^+$ and $CD11b^+$ cells

As shown in Fig. 5, we have confirmed that the number of $CD49b^+$ and $CD11b^+$ cells in the liver from IDO-KO mice treated with α-GalCer increased. Therefore, we measured the production of TNF-α on $CD49b^+$ and $CD11b^+$ cells by using intracellular cytokine staining (Fig. 6). $CD49b^+$ and $CD11b^+$ cells in the livers of both WT and IDO-KO mice significantly produced TNF-α at 12 h after α-GalCer injection. In particular, the number of TNF-α–producing cells in IDO-KO mice significantly increased compared with that in WT mice.

The IDO inhibitor 1-methyl-D-tryptophan enhances α-GalCer–induced liver injury

1-Methyl-D-tryptophan (1-MT) is a potent inhibitor of IDO, and hence we used this agent to substantiate data obtained with IDO-KO mice. WT mice were administered 1-MT orally at 0 or 5 mg/ml in drinking water for 3 d before α-GalCer stimulation. This experiment was performed twice independently. In both experiments, the serum ALT level in WT mice treated with 1-MT was significantly elevated compared with that in WT mice not treated with 1-MT at 1 d after α-GalCer stimulation (Fig. 7). Therefore,

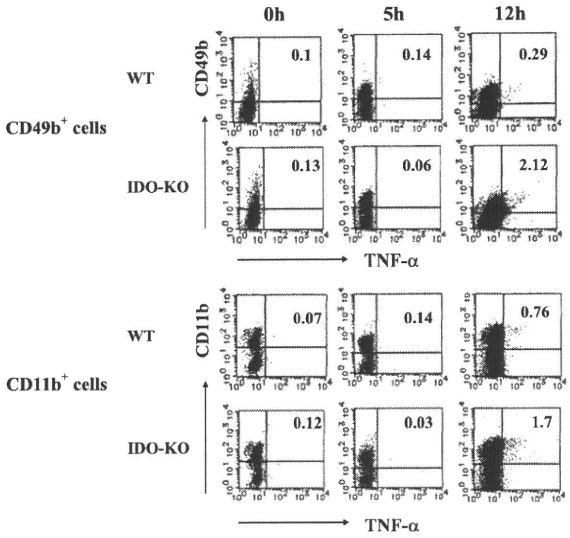

FIGURE 6. α-GalCer–induced TNF-α production in CD49b$^+$ and CD11b$^+$ cells. Flow cytometric analysis of intracellular TNF-α produced by hepatic CD49b$^+$ and CD11b$^+$ cells obtained from mice at 0, 5, and 12 h after α-GalCer injection and cultured for 4 h in brefeldin A. Data are representative of at least three independent experiments with similar results.

pharmacological inhibition of IDO with 1-MT is consistent with the exacerbated situation observed using IDO-KO mice.

Discussion

In this study, we report that α-GalCer–induced liver injury was exacerbated in IDO-KO mice, and that the exacerbation was accompanied by an increase in the number of intrahepatic TNF-α–producing MNCs. The serum ALT level was significantly augmented in IDO-KO mice compared with WT mice after α-GalCer injection. In parallel, TNF-α expression induced by α-GalCer injection was more enhanced in the livers of IDO-KO mice. Moreover, the number of intrahepatic CD49b$^+$ and CD11b$^+$ cells in IDO-KO mice treated with α-GalCer significantly increased compared with that in WT mice, and the cells from IDO-KO mice produced a large amount of TNF-α. These data indicated that deficiency of IDO increased the number of intrahepatic TNF-α–producing cells and exacerbated α-GalCer–induced liver injury. To the best of our knowledge, this is the first report describing the effects of IDO on acute hepatic injury.

IDO is an enzyme that is ubiquitously distributed in mammalian tissues and cells; that is, from L-Trp to *N*-formylkynurenine, which is further catabolized to L-Kyn. IDO production is induced by an IFN-γ–dependent and/or an IFN-γ–independent mechanism and other proinflammatory cytokines in the course of an inflammatory response in different cells, including macrophages, fibroblasts, and epithelial cells (3, 4). Previous studies on IDO have demonstrated that the role that IDO plays in regulating immune responses has been the subject of intense investigation. The bulk of the literature has focused on investigating the suppressive effects of IDO activity, predominantly on the activation of T cells (1). The prevailing theory is that IDO expressed by dendritic cells inhibits T cell activation, either directly or indirectly, by driving the development of regulatory T cells.

Inhibition of IDO activity during immune-mediated colitis has recently been reported to markedly worsen disease in the gut (19). In sharp contrast, IDO can act as a mediator of inflammatory disease, particularly in ischemia-reperfusion injury (20). Additionally, it was reported that administration of 1-MT to K/BxN mice reduced the level of inflammatory cytokines and autoantibodies, resulting in an attenuated course of arthritis (21). Thus, IDO has contrasting effects on several types of inflammation models. However, the effects of IDO function in the acute murine liver injury model remain unknown. In this study, we used the α-GalCer–induced liver injury model to examine the role of IDO an acute liver injury.

We first confirmed the expression of IDO in the liver after α-GalCer administration (Fig. 1). IDO is induced by IFN-γ and other proinflammatory cytokines, whereas such proinflammatory cytokines are secreted in mice treated with α-GalCer (15, 17). In particular, immunohistochemical examination revealed that IDO expression was enhanced in hepatocytes after α-GalCer treatment (Fig. 1*D*). These results coincide with our previous data in which murine recombinant IFN-γ induced IDO mRNA expression in primary hepatocytes in vitro (8).

In this study, using IDO-KO mice, we clearly demonstrated that the IDO deficiency caused the exacerbation of liver injury in this murine α-GalCer–induced hepatitis model (Fig. 2). As shown in Fig. 1*D*, the expression of IDO in the liver was enhanced 1 d after α-GalCer treatment, and ALT level also increased simultaneously. These results indicate that IDO expression may partially regulate the liver injury. Moreover, 1-MT, a competitive inhibitor of IDO, also exacerbated liver injury in this hepatitis model (Fig. 7). Induction of IDO by α-GalCer treatment may thus suppress the increased immune response observed in acute liver injury and attenuate the liver injury caused in this model.

Previous studies have reported that TNF-α is an important mediator in the α-GalCer–induced liver injury model (12, 22, 23). Intrahepatic NKT cells and NK cells mainly secrete TNF-α after α-GalCer injection. Although intrahepatic macrophages/monocytes are known as a pivotal source of TNF-α, they are not essential for α-GalCer–mediated hepatotoxicity (12). In this study, TNF-α production in IDO-KO mice treated with α-GalCer was increased compared with that in WT mice, and TNF-α also played a critical role in this acute liver injury model (Fig. 3). In particular, TNF-α production in CD49b$^+$ and CD11b$^+$ cells from IDO-KO mice was

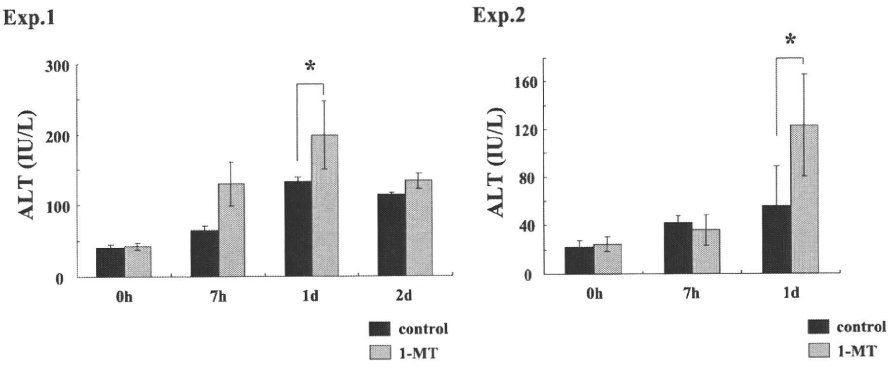

FIGURE 7. IDO inhibitor (1-MT) enhances α-GalCer–induced liver injury. IDO-WT mice were orally administered 1-MT at 0 or 5 mg/ml in drinking water for 3 d before α-GalCer stimulation. Serum ALT activity was analyzed at varying time points relative to the injection of α-GalCer into 1-MT–treated and nontreated mice. Representative charts were derived from the analyses of four or five mice per group. These experiments were independently performed twice (Exp. 1 and Exp. 2). Error bars indicate the SEM. $*p < 0.05$.

significantly increased compared with that from WT mice (Fig. 6). α-GalCer can enhance TNF-α production and cytotoxicity in NK cells and NKT cells (12, 24). The increase in the number of TNF-α–producing $CD49b^+$ cells (including NK cells and NKT cells) presumably contributes to the exacerbation of α-GalCer–induced liver injury. On the other hand, although the previous study demonstrated that macrophages/monocytes did not contribute to the progression of α-GalCer–mediated liver injury (12), TNF-α production in intrahepatic macrophages/monocytes from IDO-KO mice treated with α-GalCer was enhanced in our study. Therefore, we speculated that IDO may suppress TNF-α production in activated macrophages/monocytes.

It was previously reported that IDO induces inhibition of immune cell (e.g., NK cells and T cells) proliferation (25, 26). In our data, intrahepatic MNCs from IDO-KO mice treated with α-GalCer were apoptosis resistant with those from WT mice. Furthermore, the number of apoptotic splenocytes increased in the presence of WT hepatocytes on α-GalCer stimulation (Fig. 7). In contrast, apoptotic splenocytes did not increase in the presence of α-GalCer when splenocytes from IDO-KO mice were cultured with hepatocytes from IDO-KO mice. We suggested that activated intrahepatic MNCs may be resistant to apoptosis in the absence of IDO, and the number of intrahepatic MNCs in IDO-KO mice treated with α-GalCer increased compared with that in WT mice.

Real-time PCR analysis revealed that mRNA expression of IL-6, MIP-2, and KC in the liver of IDO-KO mice was upregulated at 24 h after α-GalCer injection (Fig. 4). There was no difference between WT and IDO-KO mice with regard to the α-GalCer reactivity, because the expression of cytokines and chemokines after α-GalCer injection was equally enhanced in the livers of WT and IDO-KO mice in the early phase (at 5 h) after α-GalCer injection. The lack of IDO promoted enhancement of IL-6, MIP-2, and KC expression in the late phase (at 24 h) after α-GalCer injection. However, there is no difference between WT and IDO-KO mice in serum MIP-2 and KC levels. These results indicated that expression of MIP-2 and KC may be affected by the expression of IDO only in the liver. Moreover, increased production of such cytokine and chemokines augments the number of intrahepatic NK cells and $CD11b^+$ cells, and they subsequently exacerbate liver injury in IDO-KO mice treated with α-GalCer. Taken together, we demonstrated that IDO inhibited not only the proliferation of NK cells and macrophages but also TNF-α production in these cells in the liver after administration of α-GalCer. IDO has the ability to suppress overactive immune response in the α-GalCer–induced hepatitis model.

In summary, this study demonstrated that IDO deficiency exacerbated liver injury in α-GalCer–induced hepatitis. IDO induced by proinflammatory cytokines may decrease the number of intrahepatic TNF-α–producing immune cells (NK cells and macrophages in particular) in acute hepatitis. Enhancement of IDO expression may suppress overactive immune response in the α-GalCer–induced hepatitis model. Accordingly, IDO regulation may be a therapeutic target in acute hepatitis.

Disclosures

The authors have no financial conflicts of interest.

References

1. Munn, D. H., E. Shafizadeh, J. T. Attwood, I. Bondarev, A. Pashine, and A. L. Mellor. 1999. Inhibition of T cell proliferation by macrophage tryptophan catabolism. *J. Exp. Med.* 189: 1363–1372.
2. Mellor, A. L., and D. H. Munn. 1999. Tryptophan catabolism and T-cell tolerance: immunosuppression by starvation? *Immunol. Today* 20: 469–473.
3. Taylor, M. W., and G. S. Feng. 1991. Relationship between interferon-γ, indoleamine 2,3-dioxygenase, and tryptophan catabolism. *FASEB J.* 5: 2516–2522.
4. Fujigaki, S., K. Saito, K. Sekikawa, S. Tone, O. Takikawa, H. Fujii, H. Wada, A. Noma, and M. Seishima. 2001. Lipopolysaccharide induction of indoleamine 2,3-dioxygenase is mediated dominantly by an IFN-γ-independent mechanism. *Eur. J. Immunol.* 31: 2313–2318.
5. Fallarino, F., U. Grohmann, K. W. Hwang, C. Orabona, C. Vacca, R. Bianchi, M. L. Belladonna, M. C. Fioretti, M. L. Alegre, and P. Puccetti. 2003. Modulation of tryptophan catabolism by regulatory T cells. *Nat. Immunol.* 4: 1206–1212.
6. Grohmann, U., F. Fallarino, R. Bianchi, C. Orabona, C. Vacca, M. C. Fioretti, and P. Puccetti. 2003. A defect in tryptophan catabolism impairs tolerance in nonobese diabetic mice. *J. Exp. Med.* 198: 153–160.
7. Terness, P., T. M. Bauer, L. Röse, C. Dufter, A. Watzlik, H. Simon, and G. Opelz. 2002. Inhibition of allogeneic T cell proliferation by indoleamine 2,3-dioxygenase-expressing dendritic cells: mediation of suppression by tryptophan metabolites. *J. Exp. Med.* 196: 447–457.
8. Iwamoto, N., H. Ito, K. Ando, T. Ishikawa, A. Hara, A. Taguchi, K. Saito, M. Takemura, M. Imawari, H. Moriwaki, and M. Seishima. 2009. Upregulation of indoleamine 2,3-dioxygenase in hepatocyte during acute hepatitis caused by hepatitis B virus-specific cytotoxic T lymphocytes in vivo. *Liver Int.* 29: 277–283.
9. Larrea, E., J. I. Riezu-Boj, L. Gil-Guerrero, N. Casares, R. Aldabe, P. Sarobe, M. P. Civeira, J. L. Heeney, C. Rollier, B. Verstrepen, et al. 2007. Upregulation of indoleamine 2,3-dioxygenase in hepatitis C virus infection. *J. Virol.* 81: 3662–3666.
10. Biburger, M., and G. Tiegs. 2008. Activation-induced NKT cell hyporesponsiveness protects from α-galactosylceramide hepatitis and is independent of active transregulatory factors. *J. Leukoc. Biol.* 84: 264–279.
11. Nakagawa, R., I. Nagafune, Y. Tazunoki, H. Ehara, H. Tomura, R. Iijima, K. Motoki, M. Kamishohara, and S. Seki. 2001. Mechanisms of the antimetastatic effect in the liver and of the hepatocyte injury induced by α-galactosylceramide in mice. *J. Immunol.* 166: 6578–6584.
12. Biburger, M., and G. Tiegs. 2005. α-Galactosylceramide-induced liver injury in mice is mediated by TNF-α but independent of Kupffer cells. *J. Immunol.* 175: 1540–1550.
13. Hoshi, M., H. Ito, H. Fujigaki, M. Takemura, T. Takahashi, E. Tomita, M. Ohyama, R. Tanaka, K. Saito, and M. Seishima. 2009. Indoleamine 2,3-dioxygenase is highly expressed in human adult T-cell leukemia/lymphoma and chemotherapy changes tryptophan catabolism in serum and reduced activity. *Leuk. Res.* 33: 39–45.
14. Ito, H., K. Ando, T. Ishikawa, K. Saito, M. Takemura, M. Imawari, H. Moriwaki, and M. Seishima. 2009. Role of TNF-α produced by nonantigen-specific cells in a fulminant hepatitis mouse model. *J. Immunol.* 182: 391–397.
15. Ito, H., K. Ando, T. Nakayama, M. Taniguchi, T. Ezaki, K. Saito, M. Takemura, K. Sekikawa, M. Imawari, M. Seishima, and H. Moriwaki. 2003. Role of Vα14 NKT cells in the development of impaired liver regeneration in vivo. *Hepatology* 38: 1116–1124.
16. Godfrey, D. I., K. J. Hammond, L. D. Poulton, M. J. Smyth, and A. G. Baxter. 2000. NKT cells: facts, functions and fallacies. *Immunol. Today* 21: 573–583.
17. Ito, H., K. Ando, T. Ishikawa, T. Nakayama, M. Taniguchi, K. Saito, M. Imawari, H. Moriwaki, T. Yokochi, S. Kakumu, and M. Seishima. 2008. Role of $V\alpha14^+$ NKT cells in the development of hepatitis B virus-specific CTL: activation of $V\alpha14^+$ NKT cells promotes the breakage of CTL tolerance. *Int. Immunol.* 20: 869–879.
18. Wintermeyer, P., C. W. Cheng, S. Gehring, B. L. Hoffman, M. Holub, L. Brossay, and S. H. Gregory. 2009. Invariant natural killer T cells suppress the neutrophil inflammatory response in a mouse model of cholestatic liver damage. *Gastroenterology* 136: 1048–1059.
19. Harrington, L., C. V. Srikanth, R. Antony, S. J. Rhee, A. L. Mellor, H. N. Shi, and B. J. Cherayil. 2008. Deficiency of indoleamine 2,3-dioxygenase enhances commensal-induced antibody responses and protects against *Citrobacter* rodentium-induced colitis. *Infect. Immun.* 76: 3045–3053.
20. Mohib, K., S. Wang, Q. Guan, A. L. Mellor, H. Sun, C. Du, and A. M. Jevnikar. 2008. Indoleamine 2,3-dioxygenase expression promotes renal ischemia-reperfusion injury. *Am. J. Physiol. Renal Physiol.* 295: F226–F234.
21. Scott, G. N., J. DuHadaway, E. Pigott, N. Ridge, G. C. Prendergast, A. J. Muller, and L. Mandik-Nayak. 2009. The immunoregulatory enzyme IDO paradoxically drives B cell-mediated autoimmunity. *J. Immunol.* 182: 7509–7517.
22. Minagawa, M., Q. Deng, Z. X. Liu, H. Tsukamoto, and G. Dennert. 2004. Activated natural killer T cells induce liver injury by Fas and tumor necrosis factor-α during alcohol consumption. *Gastroenterology* 126: 1387–1399.
23. Inui, T., H. Nakashima, Y. Habu, R. Nakagawa, M. Fukasawa, M. Kinoshita, N. Shinomiya, and S. Seki. 2005. Neutralization of tumor necrosis factor abrogates hepatic failure induced by α-galactosylceramide without attenuating its antitumor effect in aged mice. *J. Hepatol.* 43: 670–678.
24. Shimizu, K., A. Goto, M. Fukui, M. Taniguchi, and S. Fujii. 2007. Tumor cells loaded with α-galactosylceramide induce innate NKT and NK cell-dependent resistance to tumor implantation in mice. *J. Immunol.* 178: 2853–2861.
25. Frumento, G., R. Rotondo, M. Tonetti, G. Damonte, U. Benatti, and G. B. Ferrara. 2002. Tryptophan-derived catabolites are responsible for inhibition of T and natural killer cell proliferation induced by indoleamine 2,3-dioxygenase. *J. Exp. Med.* 196: 459–468.
26. Sarkhosh, K., E. E. Tredget, A. Karami, H. Uludag, T. Iwashina, R. T. Kilani, and A. Ghahary. 2003. Immune cell proliferation is suppressed by the interferon-γ-induced indoleamine 2,3-dioxygenase expression of fibroblasts populated in collagen gel (FPCG). *J. Cell. Biochem.* 90: 206–217.

Chemico-Biological Interactions 185 (2010) 247–252

Contents lists available at ScienceDirect

Chemico-Biological Interactions

journal homepage: www.elsevier.com/locate/chembioint

(−)-Epigallocatechin gallate inhibits growth and activation of the VEGF/VEGFR axis in human colorectal cancer cells

Masahito Shimizu[a,*], Yohei Shirakami[a], Hiroyasu Sakai[a], Yoichi Yasuda[a], Masaya Kubota[a], Seiji Adachi[a], Hisashi Tsurumi[a], Yukihiko Hara[b], Hisataka Moriwaki[a]

[a] Department of Internal Medicine, Gifu University Graduate School of Medicine, 1-1 Yanagido, Gifu 501-1194, Japan
[b] Tea Solution, Hara Office Inc., Tokyo, Japan

ARTICLE INFO

Article history:
Received 12 January 2010
Received in revised form 17 March 2010
Accepted 18 March 2010
Available online 25 March 2010

Keywords:
EGCG
VEGF/VEGFR axis
Colon cancer

ABSTRACT

(−)-Epigallocatechin gallate (EGCG), the major constituent of green tea, inhibits the growth of colorectal cancer cells by inhibiting the activation of various types of receptor tyrosine kinases (RTKs). The RTK vascular endothelial growth factor (VEGF)/VEGF receptor (VEGFR) axis induces tumor angiogenesis in colorectal cancer. This study examined the effects of EGCG on the activity of the VEGF/VEGFR axis and the expression of hypoxia-inducible factor (HIF)-1α, which promotes angiogenesis by elevating VEGF levels, in human colorectal cancer cells. Total and phosphorylated (i.e., activated) form (p-VEGFR-2) of VEGFR-2 proteins were overexpressed in a series of human colorectal cancer cell lines. Within 3 h, EGCG caused a decrease in the expression of HIF-1α protein and VEGF, HIF-1α, insulin-like growth factor (IGF)-1, IGF-2, epidermal growth factor (EGF), and heregulin mRNAs in SW837 colorectal cancer cells, which express a constitutively activated VEGF/VEGFR axis. A decrease was also observed in the expression of VEGFR-2, p-VEGFR-2, p-IGF-1 receptor, p-ERK, and p-Akt proteins within 6 h after EGCG treatment. Drinking EGCG significantly inhibited the growth of SW837 xenografts in nude mice, and this was associated with the inhibition of the expression and activation of VEGFR-2. The consumption of EGCG also inhibited activation of ERK and Akt, both of which are downstream signaling molecules of the VEGF/VEGFR axis, and reduced the expression of VEGF mRNA in xenografts. These findings suggest that EGCG may exert, at least in part, growth-inhibitory effects on colorectal cancer cells by inhibiting the activation of the VEGF/VEGFR axis through suppressing the expression of HIF-1α and several major growth factors. EGCG may therefore be useful in the chemoprevention and/or treatment of colorectal cancer.

1. Introduction

Neovascularization and angiogenesis play a crucial role in the growth of solid tumors. Vascular endothelial growth factor (VEGF) is the angiogenic factor most closely associated with inducing and maintaining neovascularization in cancerous tissue. VEGF binds to and activates VEGF receptors (VEGFRs), which are receptor tyrosine kinases (RTKs), and activation of the VEGF/VEGFR axis is important in pathological angiogenesis and tumor growth [1,2]. Both overexpression and activation of the VEGF/VEGFRs axis are observed in human colon cancer, and this has been shown to correlate with poor prognosis [3,4]. These reports, therefore, suggest that the specific agents that target the VEGF/VEGFR axis may be effective in reducing angiogenesis and tumor growth in colorectal cancer, and may thus improve the prognosis of patients with this malignancy. Recent clinical trials of bevacizumab, a humanized anti-VEGF monoclonal antibody, showed a survival benefit in patients with advanced colorectal cancer when combined with conventional cytotoxic chemotherapy [5].

Green tea, a commonly consumed beverage worldwide, has been studied extensively for its health benefits, including anticancer and cancer chemopreventive properties [6,7]. For instance, in patients who had colorectal adenomas removed by polypectomy, supplementation with green tea extract significantly prevented the development of metachronous colorectal adenomas [8]. Experimental studies have indicated that green tea catechins (−)-epigallocatechin gallate (EGCG), the major biologically active component of green tea, in particular, suppress cell proliferation and induce apoptosis in colon cancer cells by inhibiting the activation of various types of RTKs, including epidermal growth factor (EGF) receptor (EGFR), human epidermal growth factor receptor

Abbreviations: EGCG, (−)-epigallocatechin gallate; EGF, epidermal growth factor; EGFR, epidermal growth factor receptor; ERK, extracellular signal-regulated kinase; HER, human epidermal growth factor receptor; HIF-1α, hypoxia-inducible factor-1α; IGF, insulin-like growth factor; IGF-1R, insulin-like growth factor-1 receptor; RTK, receptor tyrosine kinase; VEGF, vascular endothelial growth factor; VEGFR, vascular endothelial growth factor receptor.

* Corresponding author. Japan. Tel.: +81 58 230 6313; fax: +81 58 230 6310.
E-mail address: shimim-gif@umin.ac.jp (M. Shimizu).

0009-2797/$ – see front matter © 2010 Elsevier Ireland Ltd. All rights reserved.
doi:10.1016/j.cbi.2010.03.036

(HER)-2 (HER2), HER3, and insulin-like growth factor (IGF)-1 receptor (IGF-1R) [9–11]. In addition, EGCG is a potent inhibitor of VEGF-dependent tyrosine phosphorylation (i.e., activation) of VEGFR-2, and this is associated with in vitro suppression of angiogenesis [12]. EGCG also suppresses the growth of human liver cancer cells by inhibiting the activation of the VEGF/VEGFR axis [13]; however, whether EGCG can inhibit the activation of this axis and thus induce the growth inhibition of colorectal cancer cells has not yet been examined.

VEGF expression is regulated by microenvironmental alterations, such as hypoxia. Recent studies have revealed that hypoxia-inducible factor (HIF)-1α, which is a key mediator of hypoxic responses, and several major growth factors, including IGF-1, EGF, and heregulin, cooperatively cause transactivation of the VEGF gene [1,14–16]. HIF-1α is also overexpressed in human colon cancers, and forced overexpression of this protein in colon cancer cells increases tumor growth and vascularization in vivo [17,18]. The present study investigated the effects of EGCG on the activation of the VEGF/VEGFR axis and the growth of colorectal cancer cells using in vitro and in vivo models, focusing especially on HIF-1α expression levels.

2. Materials and methods

2.1. Chemicals

EGCG was provided by the Mitusi Norin Co, Ltd., (Tokyo, Japan).

2.2. Cell lines and cell culture conditions

Five human colorectal cancer cell lines, Caco2, HCT116, HT29, SW480, and SW837 lines, were obtained from the American Type Culture Collection (Manassas, VA, USA) and maintained in DF10 medium containing DMEM (Invitrogen, Carlsbad, CA, USA) supplemented with 10% fetal bovine serum. The cells were cultured in an incubator with humidified air with 5% CO_2 at 37 °C.

2.3. In vivo experimental protocol

Five-week-old BALB/c nude mice (24 mice) were obtained from Charles River Japan Inc., (Tokyo, Japan). Xenograft tumors in mouse flanks were generated by the subcutaneous injection of SW837 cells, at a concentration of 5×10^6 cells per 200 μl. Seven days after tumor cell injection, the mice were randomly divided into 3 groups (8 mice per each group), each receiving treatment via drinking water: Group 1, EGCG-untreated control group (tap water); Group 2, 0.01% EGCG-treated group (tap water containing 0.01% EGCG); or Group 3, 0.1% EGCG-treated group (tap water containing 0.1% EGCG). All mice were housed in plastic cages with free access to drinking water (tap water supplemented with or without EGCG) and a pelleted basal diet, CRF-1 (Oriental Yeast Co, Ltd., Tokyo, Japan) for 35 days. A freshly prepared solution of EGCG in tap water was supplied to the experimental mice 3 times a week, and the volume of water consumed was measured during each time period. The concentrations of EGCG (0.01% and 0.1%) were established according to the findings of many previous chemopreventive studies. These doses were within the physiological range after conversion of daily intake of green tea catechins of human to mice per unit body weight [19], and were sufficient to exert anticancer properties without causing side effects in any organs [13,19–21]. The tumor size and body weight were measured every 5 days and tumor volume was calculated using the following formula: (largest diameter) × (smallest diameter)^2 × (0.5). All mice were maintained at the Gifu University Life Science Research Center, according to the Institutional Animal Care Guidelines, and the experimental protocol was approved by the Institutional Committee of Animal Experiments of Gifu University.

2.4. Protein extraction and Western blot analysis

Exponentially growing SW837 cells were serum starved for 24 h. Next, the cells were treated with 25 μg/ml EGCG for the indicated times (0, 3, 6, 12, and 24 h) in serum-free medium and total cellular protein was extracted. Total proteins were also extracted from xenografts of SW837 cells and equivalent amounts of proteins (20 (g/lane) were subjected to Western blot analysis, as described previously [11,13]. The primary antibodies for VEGFR-2, p-VEGFR-2, IGF-1R, p-IGF-1R, ERK (ERK1/2, p44/42 MAPK), p-ERK, Akt, p-Akt, and GAPDH were described previously [11,13]. The primary antibody for HIF-1α was purchased from BD Transduction Laboratories (San Jose, CA, USA). The antibody to GAPDH served as the loading control. The intensities of the blots were quantified using NIH Image software package version 1.62.

2.5. RNA extraction and quantitative real-time RT-PCR analysis

A quantitative real-time reverse transcription-PCR (RT-PCR) analysis was carried out as described previously [22]. The SW837 cells, precultured in serum-free medium for 24 h, were treated with 25 μg/ml EGCG for 3 h without serum, and total RNA was isolated using the RNAqueous-4PCR kit (Ambion Applied Biosystems, Austin, TX, USA). Total RNA was also isolated from the xenografts of SW837 cells using the same method. cDNA was generated from 0.2 (g of total RNA using the SuperScript III First-Strand Synthesis System (Invitrogen). The primers used for amplification of VEGF, HIF-1α, IGF-1, IGF-2, and GAPDH were described previously [13,23,24]. The primers used for amplification of EGF and heregulin were as follows: EGF forward, 5′-TGG GCA CAG AGC AAG GCT GC-3′; EGF reverse, 5′-TGG TGT GGT GGG TCC AGG GC-3′; heregulin forward, 5′-CAC CAC CAA GGC TGC GGG AG-3′; and heregulin reverse, 5′-GGG GCT AGC AGG GAG GCT GT-3′. Real-time PCR was performed on a LightCycler instrument (Roche Diagnostics Co, Indianapolis, IN, USA) with SYBR Premix Ex Taq (TaKaRa Bio Inc., Shiga, Japan). The expression levels of VEGF, HIF-1α, IGF-1, IGF-2, EGF, and heregulin genes were normalized to that of GAPDH gene [22].

2.6. Statistical analysis

The data are expressed as the mean ± SD. The statistical significance of the difference in mean values was tested using one-way analysis of variance (ANOVA) and unpaired *t*-test. Significance was defined as *P*-value less than 0.05. All analyses were performed using the StatView version 5.0 software program (SAS Institute, Cary, NC, USA).

3. Results

3.1. Expression of VEGFR-2 and p-VEGFR-2 proteins in human colorectal cancer cell lines

We initially examined the expression levels of VEGFR-2, the major mediator of the mitogenic and angiogenic effects of VEGFs [1,2], and phosphorylated (i.e., activated) form of VEGFR-2 protein (p-VEGFR-2) in Caco2, HCT116, HT29, SW480, and SW837 human colorectal cancer cell lines. As shown in Fig. 1, the levels of VEGFR-2 and p-VEGFR-2 proteins were markedly increased in Caco2, HCT116, SW480, and SW837 cells, in particular. These findings suggest that VEGFR-2 is overexpressed and constitutively activated in these 4 cell lines. The SW837 cell line was chosen for the following experiments because, in addition to VEGFR-2 over-

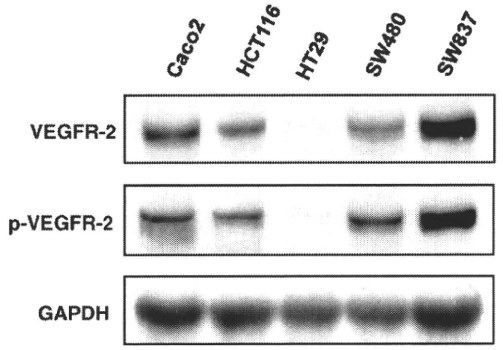

Fig. 1. The expression levels of total VEGFR-2 and p-VEGFR-2 proteins in human colorectal cancer cell lines. Total protein extracts were prepared from 70% confluent cultures of the indicated cell lines, which were maintained in DF10 medium, and equivalent amounts of protein (20 μg/lane) were examined by Western blot analysis. The antibody to GAPDH served as the loading control. Repeat Western blots gave similar results.

expression (Fig. 1), the EGFR, HER2, HER3, and IGF-1R proteins are also overexpressed and activated in this cell line [9–11].

3.2. Effects of EGCG on the expression levels of HIF-1α and on the activation of VEGFR-2, IGF-1R and their downstream signaling molecules in SW837 cells

We next examined the effects of EGCG on the expression of HIF-1α protein and on the activation of VEGFR-2 and IGF-1R proteins in SW837 cells. Time course studies have indicated that when the cells were treated with 25 μg/ml EGCG, the previously determined IC_{50} concentration [9], there was a marked decrease in the levels of VEGFR-2 and p-VEGFR-2 proteins within 6 h of treatment (Fig. 2A). Treatment with EGCG for 6 h also reduced the levels of p-IGF-1R, p-ERK, and p-Akt proteins, without having a significant effect on the total abundance of the respective proteins in SW837 cells (Fig. 2A). In contrast, the levels of HIF-1α protein were markedly decreased within 3 h of EGCG treatment (Fig. 2A). Therefore, the decrease in HIF-1α protein preceded that of the p-VEGFR-2 and p-IGF-1R proteins.

3.3. Effects of EGCG on the levels of VEGF, HIF-1α, IGF-1, IGF-2, EGF, and heregulin mRNAs in SW837 cells

Because HIF-1α and several growth factors play an important role in the transactivation of the VEGF gene [14–16], we next examined the possible effects of EGCG on the expression of VEGF, HIF-1α, IGF-1, IGF-2, EGF, and heregulin mRNAs in SW837 cells. Quantitative real-time RT-PCR analysis indicated that treatment with 25 μg/ml EGCG for 3 h significantly reduced the levels of VEGF, HIF-1α, IGF-1, IGF-2, EGF, and heregulin mRNAs ($P < 0.05$, Fig. 2B). Therefore, the expression of HIF-1α was inhibited by EGCG at both the mRNA and protein levels (Fig. 2).

3.4. Effects of EGCG on the growth of colorectal cancer xenografts

We next examined the growth-inhibitory effects of EGCG on SW837 cells using a nude mouse xenograft model. As shown in Fig. 3, drinking water with both concentrations (0.01% and 0.1%) of EGCG strongly inhibited growth of the SW837 xenografts during

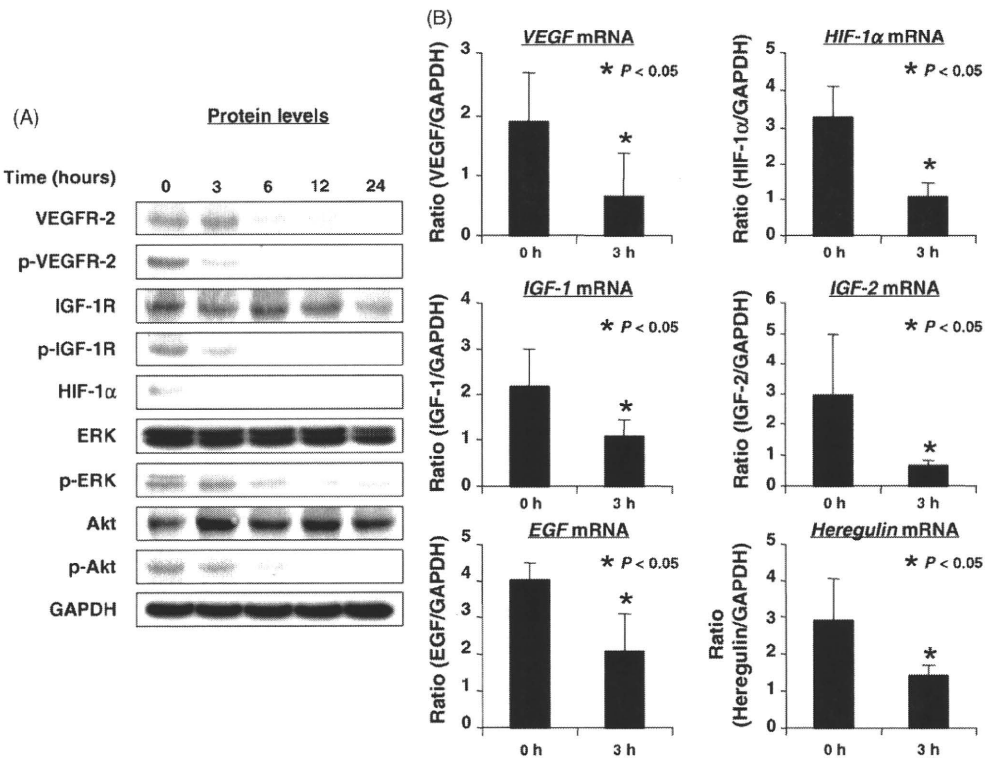

Fig. 2. Effects of EGCG on the activation of the VEGF/VEGFR and IGF/IGF-1R axes and on the cellular levels of HIF-1α in SW837 cells. (A) The SW837 cells, precultured in serum-free medium for 24 h, were treated with 25 μg/ml EGCG at 0, 3, 6, 12, and 24 h in the absence of serum. Total cellular proteins were then extracted and Western blot analysis was performed using the respective antibodies. The antibody to GAPDH served as the loading control. Repeat Western blots gave similar results. (B) The SW837 cells were precultured in serum-free medium for 24 h and treated with 25 μg/ml EGCG for 3 h without serum. Total RNA was isolated from these cells and the expression of VEGF, HIF-1α, IGF-1, IGF-2, EGF, and heregulin genes was examined by quantitative real-time RT-PCR. The expression of each gene was normalized to GAPDH. Each experiment was performed in triplicate. Bars, SD, $^*P < 0.05$.

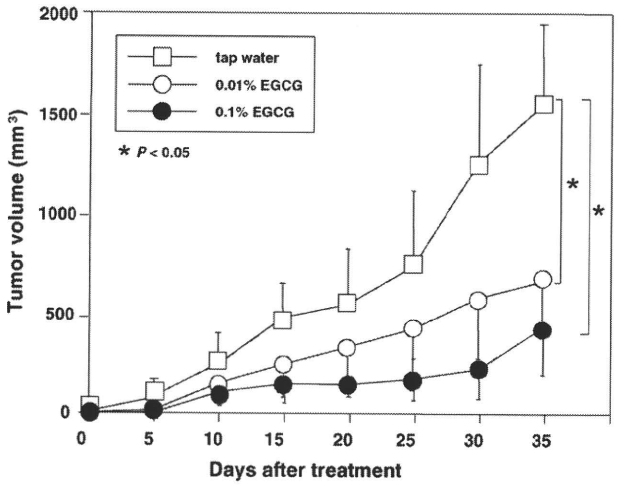

Fig. 3. Effects of EGCG on the growth of SW837 xenografts in nude mice. Male BALB/c nude mice were injected subcutaneously with 5×10^6 SW837 cells. One week after injection, the mice were divided into 3 groups and subjected to the following conditions for 35 days: Group 1, EGCG-untreated control group (tap water drinking group, □), Group 2, 0.01% EGCG drinking group (○), and Group 3, 0.1% EGCG drinking group (●). The growth curve of SW837 tumors in each group is represented. Bars, SD, $^*P < 0.05$: significant differences obtained by comparison with EGCG-untreated group.

treatment (35 days), in comparison to controls ($P < 0.05$). At the end of the study, tumor volumes were reduced by 56% and 74% in the 0.01% and 0.1% EGCG-treated groups, respectively. The average daily water intake volume did not differ between groups. Drinking water containing EGCG produced no signs of toxicity in the mice because the body weights remained stable in all groups during the experiment and no pathological alterations indicating toxicity were observed in the liver, spleen, or kidneys of the experimental mice (data not shown).

3.5. Effects of EGCG on the activation of VEGFR-2 and its downstream signaling molecules in xenografts of SW837 cells

To determine whether treatment with EGCG inhibits the activation of VEGFR-2 and its multiple downstream signaling pathways in vivo, we next examined the levels of VEGFR-2, p-VEGFR-2, p-ERK, and p-Akt proteins in EGCG-treated xenografts of SW837 cells. The expression levels of VEGFR-2 and p-VEGFR-2 proteins were decreased by consuming drinking water containing EGCG in both concentrations ($P < 0.05$, Fig. 4A). EGCG also inhibited the phosphorylation of ERK and Akt proteins in SW837 xenografts ($P < 0.05$, Fig. 4A).

3.6. Effects of EGCG on the expression of VEGF mRNA in xenografts of SW837 cells

As shown in Fig. 4B, drinking water with 0.1% EGCG caused a significant decrease in the level of VEGF mRNA in xenografts in comparison to the control mice ($P < 0.05$). Therefore, the inhibitory effect of EGCG on the expression of VEGF was observed in vivo (Fig. 4B) and in vitro (Fig. 2).

4. Discussion

There is considerable evidence that the VEGF/VEGFR axis plays a critical role in the growth of solid tumors, and therefore, it may be a potential promising target for the treatment of various types of cancers, including colorectal cancer [1,2,5]. The present study indicates that drinking water containing EGCG effectively suppresses the growth of SW837 human colorectal cancer xenografts via inhi-

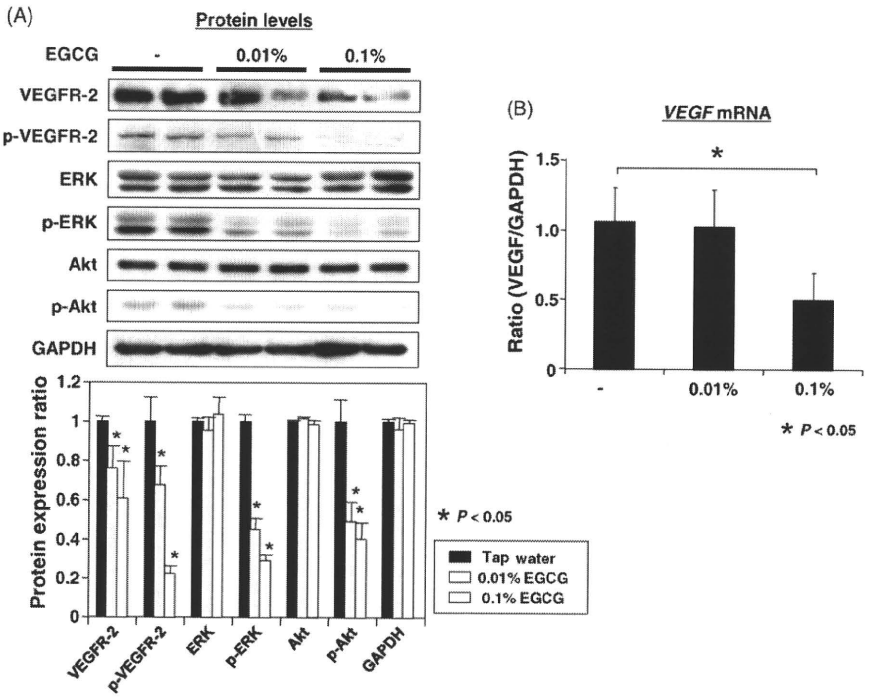

Fig. 4. Effects of EGCG on activation of the VEGF/VEGFR axis and on the cellular levels of VEGF mRNAs in SW837 xenografts. The xenografts were excised from each animal at the termination of the experiment and tumor extracts were examined by Western blot analysis using the respective antibodies (A) or by quantitative real-time RT-PCR analysis using VEGF specific primers (B). (A) The antibody to GAPDH served as the loading control. Two lanes represent protein samples from two different mice in each group (upper panel). The results obtained were quantified by densitometry and are shown in the lower panel. (B) The expression of VEGF gene was normalized to GAPDH gene expression. Bars, SD, $^*P < 0.05$: significant differences obtained by comparison with EGCG-untreated group.

bition of the VEGF/VEGFR axis (Figs. 3 and 4). The effect of EGCG on decreasing the total levels of VEGFR-2 (Figs. 2A and 4A) is a significant contributor to the inhibition of this axis. These results are consistent with a recent report that EGCG reduced expression of VEGFR-2 in human HCC cells [13]. In addition, the effect of EGCG on the levels of VEGF mRNA (Figs. 2B and 4B) also inhibits phosphorylation of VEGFR-2, because VEGF is a potent activator of VEGFRs [1,2] and reduction of p-VEGFR-2 protein expression was more apparent in comparison to that of VEGFR-2 total levels (Figs. 2A and 4A). Interference with the binding of VEGF to VEGFR and inhibition of VEGFR2 dimerization by EGCG may also inhibit VEGFR2 activation [25,26].

The present study also provides the first evidence that EGCG inhibits the expression of HIF-1α, which strongly activates VEGF expression [1] at both the mRNA and protein levels in colorectal cancer cells (Fig. 2). Because the marked decrease in cellular HIF-1α levels occurred within 3 h after the addition of EGCG and preceded the inhibition of VEGFR-2 phosphorylation (Fig. 2), we suggest that EGCG may inhibit the activation of the VEGF/VEGFR axis, in part, by suppression of HIF-1α. In addition, EGCG inhibition of HIF-1α appears to be closely associated with the inhibition of ERK and Akt phosphorylation, because HIF-1α protein synthesis is regulated by PI3K/Akt and MAPK/ERK pathway activation [1], which are also inhibited by EGCG (Fig. 2A). These findings are consistent with those of a previous report showing that EGCG decreases the levels of VEGF by suppressing HIF-1α expression and blocking the PI3K/Akt and MAPK/ERK signaling pathways, thus inhibiting the growth of liver cancer cells [13,24]. These findings also may explain the results of a previous report, which demonstrated that EGCG inhibits the induction of the VEGF promoter activity in colon cancer cells [27].

In addition to HIF-1α, several major growth factors, such as IGF-1, EGF, and heregulin, also induce the transcription of VEGF mRNA by activating a variety of RTKs and, in certain instances, these molecules cooperate with the regulation of VEGF expression [1,14–16]. For example, HIF-1α plays an important role in colorectal cancer angiogenesis by stimulating the IFG/IGF-1R related autocrine/paracrine loops [14,18,28]. These reports are significant because EGCG inhibits not only the expression of IGF-1, IGF-2, EGF, and heregulin mRNAs, but also the activation of IGF-1R and its related downstream signaling pathways in human colon cancer cells (Fig. 2). Because the PI3K/Akt pathway regulates VEGF in colon cancer cells [29], inhibition of the EGF- and IGF-activated PI3K/Akt pathway by EGCG might subsequently inhibit activation of the VEGF/VEGFR axis in the present study (Figs. 2 and 4). Drinking water with EGCG inhibited activation of the IGF/IGF-1R axis and thereby inhibited obesity-related colorectal carcinogenesis in mice [21]. In addition, the production of PGE_2, which induces VEGF expression through HIF-1α transactivation [30], is also reduced by treatment with EGCG and this is associated with inhibition of the activation of EGFR, HER2, and HER3 proteins in colon cancer cells [10]. Therefore, EGCG, which targets both HIF-1α and several RTKs, including IGF-1R, substantially inhibits activation of the VEGF/VEGFR axis (Figs. 2 and 4).

Finally, it should be emphasized that not only a high (0.1%), but also a low (0.01%) concentration of EGCG exhibited similar inhibitory effects on the growth of colorectal cancer xenografts by blocking the VEGF/VEGFR axis to the same extents (Figs. 3 and 4). Both concentrations used in the present study are considered to be physiologically relevant because the feeding protocol of EGCG at a high dose (0.1%) mimics an approximate consumption of 6 cups of green tea per day by an average adult human [19]. This point is important when considering the clinical use of this agent because a lower dose is usually associated with ensuring medical safety and thus is more acceptable for administration to patients. In fact, although the inhibition of the VEGF/VEGFR axis by bevacizumab appears to be a successful anti-angiogenic therapy, serious side effects have been reported [5]. On the other hand, while hepatotoxicity is one of the significant problems associated with green tea administration [31], even treatment with EGCG at a relatively high dose did not cause toxicity in this study. EGCG also preferentially inhibits the growth of human colorectal and liver cancer cells in comparison to normal colon epithelial cells and hepatocytes [9,23]. A recent pilot study indicated that supplementation with green tea extract significantly prevents the development of metachronous colorectal adenomas without causing serious adverse events [8]. These reports show the benefits of EGCG and encourage the clinical application of this agent for chemoprevention of colorectal cancer.

The present data (Figs. 2 and 4), combined with the findings of previous studies [9–11], indicate that EGCG inhibits not only the VEGF/VEGFR axis, but also the activation of several other RTKs, including IGF-1R, EGFR, HER2, and HER3 in colon cancer cells. Among these, VEGFR-2 is of interest because EGCG reduced both the total and phosphorylated forms of this protein (Figs. 2A and 4A). In conclusion, EGCG inhibits activation of the VEGF/VEGFR axis, at least in part, by suppressing the expression of HIF-1α and several major growth factors, supporting the potential use of this naturally occurring agent in the chemoprevention and therapy of colorectal cancer.

Conflicts of interest statement

The authors declare that no conflicts of interest exist.

Acknowledgments

This work was supported in part by Grants-in-Aid from the Ministry of Education, Science, Sports and Culture of Japan (No. 18790457 to M. S. and No. 17015016 to H. M.).

References

[1] N. Ferrara, H.P. Gerber, J. LeCouter, The biology of VEGF and its receptors, Nat. Med. 9 (2003) 669–676.
[2] L.M. Ellis, D.J. Hicklin, VEGF-targeted therapy: mechanisms of anti-tumour activity, Nat. Rev. Cancer 8 (2008) 579–591.
[3] S. Cascinu, M.P. Staccioli, G. Gasparini, P. Giordani, V. Catalano, R. Ghiselli, C. Rossi, A.M. Baldelli, F. Graziano, V. Saba, P. Muretto, G. Catalano, Expression of vascular endothelial growth factor can predict event-free survival in stage II colon cancer, Clin. Cancer Res. 6 (2000) 2803–2807.
[4] A. Giatromanolaki, M.I. Koukourakis, E. Sivridis, G. Chlouverakis, E. Vourvouhaki, H. Turley, A.L. Harris, K.C. Gatter, Activated VEGFR2/KDR pathway in tumour cells and tumour associated vessels of colorectal cancer, Eur. J. Clin. Invest. 37 (2007) 878–886.
[5] B.M. Wolpin, R.J. Mayer, Systemic treatment of colorectal cancer, Gastroenterology 134 (2008) 1296–1310.
[6] C.S. Yang, P. Maliakal, X. Meng, Inhibition of carcinogenesis by tea, Annu. Rev. Pharmacol. Toxicol. 42 (2002) 25–54.
[7] C.S. Yang, X. Wang, G. Lu, S.C. Picinich, Cancer prevention by tea: animal studies, molecular mechanisms and human relevance, Nat. Rev. Cancer 9 (2009) 429–439.
[8] M. Shimizu, Y. Fukutomi, M. Ninomiya, K. Nagura, T. Kato, H. Araki, M. Suganuma, H. Fujiki, H. Moriwaki, Green tea extracts for the prevention of metachronous colorectal adenomas: a pilot study, Cancer Epidemiol. Biomarkers Prev. 17 (2008) 3020–3025.
[9] M. Shimizu, A. Deguchi, J.T. Lim, H. Moriwaki, L. Kopelovich, I.B. Weinstein, (−)-Epigallocatechin gallate and polyphenon E inhibit growth and activation of the epidermal growth factor receptor and human epidermal growth factor receptor-2 signaling pathways in human colon cancer cells, Clin. Cancer Res. 11 (2005) 2735–2746.
[10] M. Shimizu, A. Deguchi, A.K. Joe, J.F. McKoy, H. Moriwaki, I.B. Weinstein, EGCG inhibits activation of HER3 and expression of cyclooxygenase-2 in human colon cancer cells, J. Exp. Ther. Oncol. 5 (2005) 69–78.
[11] M. Shimizu, A. Deguchi, Y. Hara, H. Moriwaki, I.B. Weinstein, EGCG inhibits activation of the insulin-like growth factor-1 receptor in human colon cancer cells, Biochem. Biophys. Res. Commun. 334 (2005) 947–953.
[12] S. Lamy, D. Gingras, R. Beliveau, Green tea catechins inhibit vascular endothelial growth factor receptor phosphorylation, Cancer Res. 62 (2002) 381–385.
[13] Y. Shirakami, M. Shimizu, S. Adachi, H. Sakai, T. Nakagawa, Y. Yasuda, H. Tsurumi, Y. Hara, H. Moriwaki, (−)-Epigallocatechin gallate suppresses the growth of human hepatocellular carcinoma cells by inhibiting activation of the vascu-

lar endothelial growth factor-vascular endothelial growth factor receptor axis, Cancer Sci. 100 (2009) 1957–1962.
[14] R. Fukuda, K. Hirota, F. Fan, Y.D. Jung, L.M. Ellis, G.L. Semenza, Insulin-like growth factor 1 induces hypoxia-inducible factor 1-mediated vascular endothelial growth factor expression, which is dependent on MAP kinase and phosphatidylinositol 3-kinase signaling in colon cancer cells, J. Biol. Chem. 277 (2002) 38205–38211.
[15] E. Laughner, P. Taghavi, K. Chiles, P.C. Mahon, G.L. Semenza, HER2 (neu) signaling increases the rate of hypoxia-inducible factor 1alpha (HIF-1alpha) synthesis: novel mechanism for HIF-1-mediated vascular endothelial growth factor expression, Mol. Cell Biol. 21 (2001) 3995–4004.
[16] H. Zhong, K. Chiles, D. Feldser, E. Laughner, C. Hanrahan, M.M. Georgescu, J.W. Simons, G.L. Semenza, Modulation of hypoxia-inducible factor 1alpha expression by the epidermal growth factor/phosphatidylinositol 3-kinase/PTEN/AKT/FRAP pathway in human prostate cancer cells: implications for tumor angiogenesis and therapeutics, Cancer Res. 60 (2000) 1541–1545.
[17] H. Zhong, A.M. De Marzo, E. Laughner, M. Lim, D.A. Hilton, D. Zagzag, P. Buechler, W.B. Isaacs, G.L. Semenza, J.W. Simons, Overexpression of hypoxia-inducible factor 1alpha in common human cancers and their metastases, Cancer Res. 59 (1999) 5830–5835.
[18] R. Ravi, B. Mookerjee, Z.M. Bhujwalla, C.H. Sutter, D. Artemov, Q. Zeng, L.E. Dillehay, A. Madan, G.L. Semenza, A. Bedi, Regulation of tumor angiogenesis by p53-induced degradation of hypoxia-inducible factor 1alpha, Genes Dev. 14 (2000) 34–44.
[19] Z.Y. Wang, R. Agarwal, D.R. Bickers, H. Mukhtar, Protection against ultraviolet B radiation-induced photocarcinogenesis in hairless mice by green tea polyphenols, Carcinogenesis 12 (1991) 1527–1530.
[20] S. Gupta, K. Hastak, N. Ahmad, J.S. Lewin, H. Mukhtar, Inhibition of prostate carcinogenesis in TRAMP mice by oral infusion of green tea polyphenols, Proc. Natl. Acad. Sci. U.S.A. 98 (2001) 10350–10355.
[21] M. Shimizu, Y. Shirakami, H. Sakai, S. Adachi, K. Hata, Y. Hirose, H. Tsurumi, T. Tanaka, H. Moriwaki, (−)-Epigallocatechin gallate suppresses azoxymethane-induced colonic premalignant lesions in male C57BL/KsJ-db/db mice, Cancer Prev. Res. 1 (2008) 298–304.
[22] Y. Yasuda, M. Shimizu, H. Sakai, J. Iwasa, M. Kubota, S. Adachi, Y. Osawa, H. Tsurumi, Y. Hara, H. Moriwaki, (−)-Epigallocatechin gallate prevents carbon tetrachloride-induced rat hepatic fibrosis by inhibiting the expression of the PDGFRbeta and IGF-1R, Chem. Biol. Interact. 182 (2009) 159–164.
[23] M. Shimizu, Y. Shirakami, H. Sakai, H. Tatebe, T. Nakagawa, Y. Hara, I.B. Weinstein, H. Moriwaki, EGCG inhibits activation of the insulin-like growth factor (IGF)/IGF-1 receptor axis in human hepatocellular carcinoma cells, Cancer Lett. 262 (2008) 10–18.
[24] Q. Zhang, X. Tang, Q. Lu, Z. Zhang, J. Rao, A.D. Le, Green tea extract and (−)-epigallocatechin-3-gallate inhibit hypoxia- and serum-induced HIF-1alpha protein accumulation and VEGF expression in human cervical carcinoma and hepatoma cells, Mol. Cancer Ther. 5 (2006) 1227–1238.
[25] T. Kondo, T. Ohta, K. Igura, Y. Hara, K. Kaji, Tea catechins inhibit angiogenesis in vitro, measured by human endothelial cell growth, migration and tube formation, through inhibition of VEGF receptor binding, Cancer Lett. 180 (2002) 139–144.
[26] S.K. Rodriguez, W. Guo, L. Liu, M.A. Band, E.K. Paulson, M. Meydani, Green tea catechin, epigallocatechin-3-gallate, inhibits vascular endothelial growth factor angiogenic signaling by disrupting the formation of a receptor complex, Int. J. Cancer 118 (2006) 1635–1644.
[27] Y.D. Jung, M.S. Kim, B.A. Shin, K.O. Chay, B.W. Ahn, W. Liu, C.D. Bucana, G.E. Gallick, L.M. Ellis, EGCG, a major component of green tea, inhibits tumour growth by inhibiting VEGF induction in human colon carcinoma cells, Br. J. Cancer 84 (2001) 844–850.
[28] D. Feldser, F. Agani, N.V. Iyer, B. Pak, G. Ferreira, G.L. Semenza, Reciprocal positive regulation of hypoxia-inducible factor 1alpha and insulin-like growth factor 2, Cancer Res. 59 (1999) 3915–3918.
[29] S. Cascio, R. Ferla, A. D'Andrea, A. Gerbino, V. Bazan, E. Surmacz, A. Russo, Expression of angiogenic regulators, VEGF and leptin, is regulated by the EGF/PI3K/STAT3 pathway in colorectal cancer cells, J. Cell. Physiol. 221 (2009) 189–194.
[30] R. Fukuda, B. Kelly, G.L. Semenza, Vascular endothelial growth factor gene expression in colon cancer cells exposed to prostaglandin E2 is mediated by hypoxia-inducible factor 1, Cancer Res. 63 (2003) 2330–2334.
[31] J.D. Lambert, M.J. Kennett, S. Sang, K.R. Reuhl, J. Ju, C.S. Yang, Hepatotoxicity of high oral dose (−)-epigallocatechin-3-gallate in mice, Food Chem. Toxicol. 48 (2010) 409–416.

HSP90 inhibitors induce desensitization of EGF receptor via p38 MAPK-mediated phosphorylation at Ser1046/1047 in human pancreatic cancer cells

SEIJI ADACHI[1,2], ICHIRO YASUDA[1], MASANORI NAKASHIMA[1], TAKAHIRO YAMAUCHI[1], JUNICHI YAMAUCHI[2], HIDEO NATSUME[2], HISATAKA MORIWAKI[1] and OSAMU KOZAWA[2]

Departments of [1]Gastroenterology and [2]Pharmacology, Gifu University Graduate School of Medicine, Gifu 501-1194, Japan

Received December 21, 2009; Accepted February 9, 2010

DOI: 10.3892/or_00000815

Abstract. Heat shock protein (HSP) 90 is known to be a molecular chaperone whose association is required for the stability and function of oncogenic protein including epidermal growth factor receptor (EGFR) that promotes cancer cell growth. Therefore, HSP90 is a promising target for therapy against cancer including in the pancreas, some of which are highly dependent on EGFR. We investigated the effects of HSP90 inhibitors on cytotoxicity and desensitization of EGFR in human pancreatic cancer cells (KP3, BxPc3 and AsPc1). 17-allylamino-17-demethoxy-geldanamycin (17-AAG), an inhibitor of HSP90, caused desensitization of EGFR in a time-dependent manner, concurrently inducing phosphorylation of EGFR at Ser1046/1047 (Ser1046/7), a site which plays an important role in EGFR desensitization in these pancreatic cancer cells. We also found similar effects in KP3 cells treated with other HSP90 inhibitors, geldanamycin and 17-dimethylamino-ethylamino-17-demethoxy-geldanamycin (17-DMAG). In KP3 cells, 17-AAG induced activation of either p44/p42 mitogen-activated protein kinase (MAPK) or p38 MAPK. Interestingly, whereas the inhibition of p44/p42 MAPK attenuated neither phosphorylation of EGFR at Ser1046/7 nor desensitization of EGFR, the phosphorylation at Ser1046/7 induced by 17-AAG was markedly attenuated by the inhibition of p38 MAPK, indicating that p38 MAPK induced this phosphorylation. Moreover, the inhibition of p38 MAPK significantly attenuated 17-AAG-induced EGFR desensitization. These results strongly suggest that EGFR phosphorylation at Ser1046/7 via activation of p38 MAPK induced by HSP90 inhibitors plays a pivotal role in EGFR desensitization in human pancreatic cancer cells.

Correspondence to: Dr Seiji Adachi, Department of Gastroenterology, Gifu University Graduate School of Medicine, Gifu 501-1194, Japan
E-mail: seijiadachi0123@gmail.com

Key words: HSP90, EGFR, desensitization, p38 MAPK, pancreatic cancer

Introduction

Pancreatic cancer is a highly lethal disease that is usually diagnosed at a late stage and is not amenable to surgery. The overall 5-year survival rate for pancreatic cancer patients is only 4% due to the lack of treatment options (1). Gemcitabine is currently considered to be the standard of care for the treatment of advanced pancreatic cancer. Moreover, in clinical trials, combination of gemcitabine with certain other cytotoxic drugs, including cisplatin, oxaliplatin, capecitabine, and 5-fluorouracil have been undertaken, but all have failed to provide substantial increases in survival benefit (2).

The receptor tyrosine kinase (RTK) family of cell surface receptors includes the epidermal growth factor receptor (EGFR) and its relatives ErbB2/HER2, ErbB3/HER3 and ErbB4/HER4. In general, binding of ligand to EGFR leads to receptor dimerization, autophosphorylation and activation of several downstream signaling pathways, which upon activation lead to cell proliferation, motility and enhanced survival (3). Expression of EGFR is known to be over-expressed in pancreatic adenocarcinoma (4). EGFR activation reportedly has the ability to transform normal cells to a neoplastic phenotype when it is expressed at a high level or when an activated mutation is introduced into it (5,6). Therefore, activation of EGFR appears to have an important role in the growth and progression of many types of cancers including pancreas and the EGFR-mediated pathway is one of the most promising targets for the development of new strategies in anti-cancer treatments. Agents capable of inhibiting EGFR activity which results in the suppression of cell proliferation and angiogenesis have significant potential for use in chemotherapy for the treatment of multiple malignancies (4). Increasing evidence shows the efficacy of EGFR-targeted agents, including monoclonal antibodies on the one hand, which are registered for metastatic colorectal cancer (7), and tyrosine kinase inhibitors on the other, which have been available for advanced lung cancer (8).

It is generally recognized that heat shock proteins (HSPs) function as molecular chaperones in protein folding, oligomerization and translocation and are often found to be over-expressed in many types of cancers. Among them, HSP90 is an abundant molecular chaperone and represents 1-2% of

total cellular protein, which increases to 4-6% under stress (9). HSP90 is a molecular chaperone whose association is required for the stability and function of multiple mutated, chimeric and overexpressed signaling proteins that promote the growth and/or survival of cancer cells. The N-terminal domain contains a unique nucleotide binding pocket that binds both ATP and ADP. Conformational changes that occur upon binding and hydrolysis of ATP regulate the ability of the chaperone to bind its client proteins (10). HSP90 client proteins include, HER-2 (11), p53, MAPK/Erk, Akt (12), the transcription factor HIF-1α (13), and mutated EGFR (14). Chaperone activity is also regulated by the binding of co-chaperone proteins including Hsp70, Hip, Hop, CDC37/p50, immunophilins and Aha1 (10,15).

HSP90 inhibitors, by interfering ATP binding, cause the destabilization and eventual degradation of HSP90 client proteins. Among HSP90 inhibitors, 17-allylamino-17-demethoxygeldanamycin (17-AAG), is currently in completing phase I/II clinical trials as a single agent cancer therapeutic (16). As for EGFR, it has been shown that L858R and deletion mutant EGFR proteins found in non-small cell lung cancer cells interact with the chaperone and are more sensitive to degradation following HSP90 inhibition than wild-type EGFR (14).

Receptor desensitization is the most prominent regulatory system of EGFR signal attenuation and involves the internalization and subsequent degradation of the activated receptor in the lysosomes (17). With the current knowledge of the mechanism underlying EGFR desensitization, this molecular event seems to involve several important phosphorylation sites. One is the phosphorylation at Tyr1045, which provides a docking site for the ubiquitin ligase c-Cbl resulting in ubiquitination of the EGFR (18) and the others are the phosphorylation at serine or threonine residues, which are thought to represent a mechanism for attenuation of the receptor kinase activity (19,20). Among the major sites of serine and threonine phosphorylation of the EGFR, it has previously been shown that the serine 1046/1047 (Ser1046/7) phosphorylation sites are required for EGFR desensitization in EGF-treated cells (21). Moreover, mutations of Ser1046/7 are reported to cause a marked inhibition of the EGF-stimulated endocytosis and desensitization of cell surface receptors (20). In addition, we have recently reported that p38 mitogen-activated protein kinase (MAPK) controls EGFR desensitization via phosphorylation at Ser1046/7 (22), suggesting that serine phosphorylation of EGFR or p38 MAPK activation might be considered a new therapeutic target especially to counter cancer cells of the colon, lung, pancreas and breast that highly express EGFR.

In this study, we investigated the anti-cancer effects of HSP90 inhibitors, focusing on the EGFR desensitization and its mechanism in human pancreatic cancer cells. HSP90 inhibitors caused desensitization of EGFR mediated by its phosphorylation at Ser1046/7 via activation of p38 MAPK in these cells.

Materials and methods

Cell culture and chemicals. Human pancreatic cancer cells were grown in Roswell Park Memorial Institute (RPMI)-1640 (Invitrogen, San Diego, CA), containing 10% fetal calf serum (FCS) as described previously (23). Geldanamycin was purchased from Invivogen, Sigma Chemicals Co. (St. Louis, MO). SB203580, PD98059, 17-AAG and 17-dimethylamino-ethyl-amino-17-demethoxygeldanamycin (17-DMAG) were purchased from Calbiochem-Novabiochem Corporation (La Jolla, CA), respectively. They were solubilized in DMSO. BIRB0796 was obtained from Dr Philip Cohen (University of Dundee, UK).

Cell viability assays. Cell viability assay was performed using the 3-(4,5-dimethylthiazol-2-yl)-2,5-diphenyltetrazolium bromide (MTT) cell proliferation kit I (Roche Diagnostics Co., Indianapolis, IN), according to the instructions of the manufacturer. In brief, pancreatic cancer cell lines were plated onto 96-well plates ($3x10^3$ cells/well) and 24 h later, the cells were treated with the indicated doses (0-1000 nM) of the indicated compounds for 72 h in RPMI-medium containing 10% FCS. The medium and drugs were not changed during this time period. All assays were done in triplicate.

Western blot analysis. The cells were lysed in lysis buffer [20 mM Tris (pH 7.5), 150 mM NaCl, 1 mM EDTA, 1 mM EGTA, 1% Triton X-100, 2.5 mM sodium pyrophosphate, 50 mM NaF, 50 mM HEPES, 1 mM Na_3VO_4 and 2 mM phenylmethylsulfonyl fluoride (PMSF)] and scraped from the Petri dishes. Protein extracts were then examined by Western blot analysis as previously described (24). The antibodies used in these studies were anti-EGFR, anti-GAPDH (Santa Cruz Biotechnology, Santa Cruz, CA), anti-phospho-EGFR (Ser1046/7), anti-p44/p42 MAPK, anti-phospho-p44/p42 MAPK, anti-phospho-p38 MAPK, anti-p38 MAPK, anti-phospho-stress-activated protein kinase/c-Jun-N-terminal kinase (SAPK/JNK) and anti-SAPK/JNK (Cell Signaling, Beverly, MA). Anti-mouse IgG or anti-rabbit IgG antibodies (Amersham Pharmacia Biotech, Buckinghamshire, UK) were used as the secondary antibodies. Each membrane was developed using an enhanced chemiluminescence detection system (Amersham Pharmacia Biotech).

Statistical analysis. Quantitative analysis of the indicated protein band was calculated as follows; the background was first subtracted from the signal intensity (total optical density) of each protein signal and then each value was normalized with GAPDH or total protein and expressed as relative signal intensity with respect to the respective control. The data are presented as the mean ± SEM of triplicate determinations, and analyzed by ANOVA followed by the Bonferroni method for multiple comparisons between pairs. A $p<0.05$ was considered statistically significant.

Results

HSP90 inhibitors exert anti-proliferative effects in human pancreatic cancer cells. It has previously been reported that overexpression of EGFR in pancreatic cancers has an important role in its aberrant growth and progression (4). We first performed cell proliferating assay using MTT to examine the anti-cancer effects of 17-AAG, an HSP90 inhibitor, in BxPc3, AsPc1 and KP3 pancreatic cells. As